Analysis of Thermal Behaviour of a Microprocessor Using Simulation and Experiment

Dissertation submitted in partial fulfilment of the requirements

for the award of degree

of

Master of Technology in Marine Engineering and Management

By

NAVEEN M

(Reg. No. 2101215002)

Under the guidance of

DR. NACHIKETA DAS

DR. SABYASACHI MONDAL

DR. DEEPAK MISHRA

Department of Marine Engineering

INDIAN MARITIME UNVERSITY

(A Central University, Government of India)

Indian Maritime University Kolkata Campus

Kolkata – 700088

July 2023

Department of Marine Engineering
INDIAN MARITIME UNVERSITY
(A Central University, Government of India)
KOLKATA -700088, INDIA

CERTIFICATE

This is to certify that the thesis entitled **" Analysis of Thermal Behaviour of a Microprocessor Using Simulation and Experiment "** submitted by **Mr. Naveen M (2101215002)** of the Department of Marine Engineering, Indian Maritime University (Kolkata Campus), in partial fulfilment of the requirements for the award of the degree of **Master of Technology** in Marine Engineering and Management, is a record of bonafide research work carried out under my supervision and guidance.

The content of the thesis does not form a basis for the award of other degree to him at the best of my knowledge. The thesis in my opinion, is worthy of consideration for the award of the degree of **Master of Technology** in Marine Engineering and Management in accordance with regulation of the institute.

Dr. Nachiketa Das	**Dr. Sabyasachi Mondal**	**Dr. Deepak Mishra**
Supervisor	Supervisor	Supervisor, Course Coordinator
Indian Maritime University	Amity University	Indian Maritime University
Kolkata Campus	Kolkata Campus	Kolkata Campus
Kolkata – 700888, India	Kolkata – 700135, India	Kolkata – 700888, India

COPYRIGHT AND CONSENT FORM

To ensure uniformity of treatment among all contributors, other forms may not be substituted for this form, nor may any wording of the form be changed. This form is intended for original material submitted to the Indian Maritime University, Kolkata Campus [IMU KC], Kolkata. must accompany any such material in order to be published by the Indian Maritime University, Kolkata Campus [IMU KC], Kolkata. Please read the form carefully and keep a copy for your files.

TITLE OF THESIS: Analysis of Thermal Behaviour of a Microprocessor Using Simulation and Experiment

AUTHOR'S NAME and ADDRESS: NAVEEN M, Myalil Puthanpurayil (H), Ganganagar, Chettarickal, Near NSS School, Koratty South, Thrissur, Kerala, Pin – 680308, India

COPY RIGHT TRANSFER

1. The undersigned hereby assigns to Indian Maritime University, Kolkata Campus. all rights under copyright that may exist in and to: (a) the above Work. including any revised or expanded derivative works submitted to the IMU KC by the undersigned based on the work and (b) any associated written or multimedia components or other enhancements accompanying the work.

CONTENT AND RELEASE

2. In the event the undersigned makes a presentation based upon the work at a conference hosted or sponsored in whole or in part by the IMU KC, the undersigned, in consideration for his/her participation in the conference, hereby grants the IMU KC the unlimited, worldwide, irrevocable permission to use, distribute, publish, license, exhibit, record, digitize, broadcast, reproduce and archive; in any format or medium, Whether now known or hereafter developed: (a) his /her presentation and comments at the conference: (b) any written materials or multimedia files used in connection with his/her presentation and; (c) any recorded interview him/her (collectively, the “Presentation"). The permission granted includes the transcription and reproduction of the Presentation for inclusion in products sold or distributed by IMU KC and live or recorded broadcast of the Presentation during or after the conference.

3. In connection with the permission granted in Section 2, the undersigned hereby grants IMU KC the unlimited, worldwide, irrevocable right to use his/her name, picture, likeness, voice and biographical information as part of the advertisement, distribution and sale of products incorporating the Work or Presentation, and releases IMU KC from any claim based on right of privacy or publicity.
4. The undersigned hereby warrants that the Work and Presentation (collectively, the "Materials") are original and that he/she is the author of the Materials. To the extent the Materials incorporate test passages, figures, data or other material from the works of others, the undersigned has obtained any necessary permissions.

GENERAL TERMS

- The undersigned represents that he/she has the power and authority to make and execute this assignment.
- The undersigned agrees to indemnify and hold harmless the IMU KC from any damage or expense that maar arise in the event of a breach of any of the warranties set forth above.
- In the event the above work is not accepted and published by the IMU KC or is withdrawn by the author(s) before acceptance be the IMU KC, the foregoing copyright transfer shall become null and void said all materials embodying the work submitted to the IMU KC will be destroyed.
- For jointly authored works, all joint authors should sign, or one of the authors should sign as authorized agent for the others.

Signature of the Author

DECLARATION

I certify that

a. The work contained in this thesis is original and has been done by me under the guidance of my supervisors.

b. The work has not been submitted to any other Institute for any degree or diploma.

c. I have followed the guidelines provided by the Institute in preparing the thesis.

d. I have conformed to the norms and guidelines given in the Ethical Code of Conduct of the Institute.

e. Whenever I have used materials (data, theoretical analysis, figures, and text) from other sources, I have given due credit to them by citing them in the text of the thesis and giving their details in the references. Further, I have taken permission from the copyright owners of the sources, whenever necessary.

.....

Signature

.....

Date

ACKNOWLEDGEMENT

It is my proud privilege to acknowledge the kind of help and guidance received from faculties in preparation of this report. It would not have been possible to prepare this report in this form without their valuable help, cooperation and guidance. I am expressing my sincere gratitude to our beloved Director of IMU Kolkata Campus Rear Admiral (Retd.) Rangachari P J for his constant support and encouragement and making library and laboratory facilities available in preparation of this report.

I would like to thank Lecturer, Dr. Nachiketa Das, Department of Marine Engineering and Assistant Professor, Dr. Sabyasachi Mondal (Amity University Kolkata) for their guidance throughout the period of the project. I would also like to thank Dr. Deepak Mishra, Course Coordinator (M. Tech - MEM), for his motivation and support for completion of the project.

Last but not the least, I take this opportunity to thank all faculty members of Marine Department for their help and encouragement.

Table of Contents

LIST OF FIGURES

LIST OF TABLES

LIST OF ABBREVIATIONS AND SYMBOLS

ABBREVIATIONS

CPU – Central Processing Unit

HS1 – Heatsink 1 (Big)

HS2 – Heatsink 2 (Small)

SYMBOLS

Q_{conv} – Convective heat transfer

h – Heat transfer coefficient

A – Area for heat transfer

T_b – Body temperature

T_a – Ambient temperature

V, u – Velocity

P, p – Pressure

ρ – Density

μ - Dynamic viscosity

Fi - External Force

T - Temperature

cp - Specific heat capacity

k - Thermal conductivity

φ - Rate of internal heat generation per unit volume

ABSTRACT

Thermal management of microprocessor is considered as an important factor in computer appliances. Several analysis and methods have been discussed regarding the scope of heat sink and microprocessor. The shape, size, material of heat sink and velocity and direction of air from the CPU fan plays an important role for thermal management of microprocessor while running the CPU. In this research a numerical and experimental analysis is done for the heat sink and microprocessor in order to understand the thermal response. Numerical analysis is done using software ANSYS 2023 STUDENT R1 version and an infrared thermographic study has been done as part of experimental analysis on the CPU model HP COMPAQ ELITE 8300 SFF. Microprocessor used in this experiment is Intel core i7 chips and exact dimension of CPU chassis have been taken for the numerical part. The thermal images are captured with Fluke Ti 450 camera. The device offers high spectral resolution while taking the thermal image. Analysis shows there are small deviations between the numerical and experimental part. Using nanofluids, a method is also been discussed for thermal management of microprocessor as a substitute for heat sink, for future scope of the project.

Keywords: Microprocessor, Heat sink, Thermal image camera, CPU chassis, Nanofluids

CHAPTER 1

INTRODUCTION

Damage to the microprocessor of a CPU has become a common issue in recent years as a result of usage. It is important to note that the temperature levelling of the microprocessor is dependent on the heat sink installed above the microprocessor. Microprocessor temperature levelling is affected by the shape and material of the heatsink, the direction and velocity of the airflow from the CPU fan, and the gap between the fan and the installed heatsink. Thermal analysis, temperature levelling, and heat dissipation are becoming increasingly important in the production of microprocessors and electronic chips. Many studies and research have been conducted on microprocessors and heat sinks.

1.1. Literature Review

Hamadeh and Al-Habaibeh [1] used the infrared thermal image method and mathematical modelling to perform thermal characterization of embedded electronics in E-Textiles. LEDs, sensors, and batteries are only a few examples of the electronics used in e-textiles that are fixed within the yarn. This study examines the temperature distribution of LEDs in their embedded, encased, and bare phases during the E-yarns production process using infrared thermographic imaging technology. The results of this research showed that an appropriate lens may be used to get knowledge regarding the thermal properties of smart textiles using an infrared thermal imaging approach. Yamada et al. [2] used a thermal network model and Bayesian optimization (BO) to examine thermal design optimization of electronic circuit board arrangement utilizing transient heating chips. They provided details of a technique that combines lumped capacitance thermal network modelling with Bayesian optimization (BO) to optimize the thermal design of such circuit boards. An experiment was conducted by Leon et al. [3] to enhance shipboard electronics cooling by heat sink design optimization. Using perforated fins, they examined how perforation geometry affected the qualities of laminar airflow and heat transmission. The results show that for perforated fins with a certain heat transfer surface area, circular perforations are the most effective. An experimental study was done by Kai et al. [4] to determine the impact of heat sink temperature on the functional properties of a novel kind of loop heat pipe. They concluded that when a loop heat

pipe system is used in electric cooling, it can successfully operate in a wide range of heat sink temperatures. To ascertain the impact of design on the thermal response of press-fit diodes, Moure et al. [5] carried out infrared thermographic research. This work has components that link the design and heat release from power dissipation. Sanchez et al. [6] used confocal Raman microscopy to examine the temperature behaviour of active Si in press-fit rectifier diodes. Applications of artificial intelligence and machine learning for thermally aware SoC architectures were studied by Norman et al. [7]. The results are outstanding and show a tremendous amount of room for thermal advancements, which immediately translate into better product performance. Tilli et al. [8] investigated a two-layer distributed model predictive control approach for thermal control of a system-on-chip multiprocessor. They then present a method for constructing an efficient distributed MPC using approximated but effective modular thermal models. Yan et al. [9] investigated the use of a micro heat sink to improve thermal management in electronic devices. To eliminate unequal temperature distribution, this article introduces current thermal improvement methods in micro heat sinks.

For multicore processors, Zhang et al. [10] tested hot spot-aware thermoelectric array-based cooling. The numerical results on an Intel chip showed that, as compared to the conventional passive heat sink cooling methods, the suggested TEC-Array cooling technology may dramatically lower temperatures. Researcher Yan et al. [11] investigated integrated gradient distribution annular cavity micro pin fin heat management to control the heat produced by 3D devices with uneven hotspots. Novel gradient distribution annular-cavity pin fins were created to handle considerable numerous heat flux settings in order to maximize heat transfer area and remove flow dead zones. Utilizing a two-sided, symmetrical intake cavity, coolant from the micro-channel rushes into the middle cavity, creating local acceleration that affects the following pin-fins.

Nishi [12] investigated a steady-state small thermal model for a microprocessor package that replicates transient thermal spreading resistance using three-dimensional simulation. The optimization of a longitudinal porous fin and transient thermal analysis subjected to a conductive-convective-radiative process and magnetic field have been studied by Oguntala et al. [13]. The finite volume method is utilized to solve the designed model. The particle swarm optimization technique is used to optimize key fin performance parameters. They found that raising the thermal conductivity factor enhanced heat transmission from the base to the bottom of the fin, which

affected the radiative diffusion procedure. Hassan et al. [14] conducted a study on thermal peaks in the system on chips (SoC). The experiment outlines a technique for keeping track of thermal peaks, which are significant issues when developing integrated circuits for a range of cutting-edge technologies. An array of oscillators is used to detect thermal peaks. The experiments were carried out by Smolentsev et al. [15] using a microprocessor temperature control system for a thermal item. They determined that their efforts would enable them to design microprocessor-based temperature controllers for use in a variety of regulators. For use in microprocessor applications, Pedro et al. [16] investigated the thermal and electrical properties of an inductor-based ANPC-Type Buck converter.

Ferdows et al. [17] use ANSYS CFX software to numerically study and model a plate-fin heat sink with a horizontal orientation of fin and a chassis of computer. They proved that a heat sink's fin position affects how fluid flows through the chassis. Jaffri and Tijani [18] examined how perforated pin fins affect a heat sink's thermal performance when forced convection is present. They found that perforated flat plate heat sinks and pin fins had higher thermal efficiency than solid flat plate heat sinks. Research on the thermos-electric air cooler module for two processor workstation computers is being done experimentally by Naphon et al. [19]. The CPU and air temperatures of the dual- computer processor is found to be significantly influenced by the thermo-electric air cooler module. The air distribution within the computer chassis is also significantly impacted by the working modes, sizes, and positions of the cooling fan.

A short heat pipe cooling system was used by Wiriyasrt et al. [20] to study the heat management system of processors. The common cooling system is used to examine the fluctuations in processor temperature caused by the cooling system of heat pipe. The physical characteristics of working fluids and heat pipe inclination angles have a major impact on cooling capacity, resulting in changes in CPU temperature. In comparison to a heat pipe without porous material, one with porous media reduces the CPU temperature. Chang et al. [21] used computational fluid dynamics to analyze channel geometry impact on heat transmission as well as fluid flow properties of microchannel heatsinks having rectangular grooves in the various curved ribs and sidewalls in the center basic flow. The findings suggested that the use of ribs and grooves together might greatly improve overall performance. To analyze the thermal behaviour and thermal viability of several kinds of microprocessors (2D, M3D, and TSV-3D (“Through-silicon-via based 3D”)) with various

cooling techniques, Amrouch et al. [22] designed an integrated framework. In comparison to the 2D microprocessor, their investigation reveals that the optimal M3D microprocessor configuration generated the greatest outcomes.

For communication between IP cores in NoC-based SoCs, Mishra and Charles [23] suggested a minimal encryption and anonymous routing protocol. Their method utilizes a unique secret-sharing technique to reduce the significant cost associated with conventional encryption and anonymous routing protocols while guaranteeing the required security objectives are achieved. According to experimental findings, current security methods on NoC may cause a large (1.5X) performance deterioration, but our technique offers the same security features with a negligible (4%) performance effect. Li et al. [24] done experimental and numerical studies to compare the performance of 3D piled chips with/without longitudinal vortex generators in the gap. The performance of heat and flow transmission at different mass flow rates, heating power, and LVG spacing are explored. The results of the experiments and the numerical analysis demonstrated that the LVGs array may enhance the cooling capability of the chip with a micro gap. A commercial thermoelectric module was used in an experiment by Saber and Al-Shehri [25] to investigate its capacity to cool hotspots in chips at various heat rates. The findings demonstrated that at high heat rates compared to low heat rates, the optimal electrical current was continuously greater.

To enhance the cooling capability of PC processor, Abdelillah A. Belarbi1, M'hamed Beriache, and Ahmed Bettahar [26] carried out an experimental assessment of the aerodynamic and thermal efficiency of a rectangular mini-channel heatsink exposed to an impinging air jet. The findings indicate that for a given value, a ratio of "height jet/diameter" offers improved cooling and that a longitudinal heat source displacement from a given distance enhances cooling effectiveness. Krishnayatra et al. [27] investigated the thermal efficiency of fins for a new axial finned-tube heat exchanger and made predictions utilizing the ML regression approach. It has been examined and researched how variations in fin thickness, or spacing, convective heat transfer coefficient, and material affect overall effectiveness and efficiency. The findings have been analyzed with regard to temperature profiles of different form profiles. The efficiency was shown to increase with fin thickness and decrease with fin spacing. Tabish Alam et al. [28] presented a new microchannel heat sink design that can handle the heat load (dissipation of excessive heat) and keeps the MHS temperature within a safe range. In laminar flow, the impact of circular projecting ribs with sector

angles ranging from 45° to 80° was investigated. It was discovered that the circular protrusion ribs 80° sector angle had the highest value of the Nusselt number, which ranged from 7.26 to 64.11. The effects of applying an uneven heat transfer coefficient profile over the convective surface of an integrated processor heatsink as a possible better cooling idea were examined by Robinson et al. [29]. To represent a typical contemporary high-performance CPU, a finite element model with thick copper heatsinks and a centered heat source at a certain degree of heat flux was examined. Next, a heat transfer coefficient with a Gaussian and uniform distribution was taken into account. The maximum temperature difference, maximum temperature, and average temperature were the three source temperature objectives that were optimized using single and multi-objective genetic algorithms. The research revealed that the multi-objective optimization approach produced the optimal distribution of heat transfer coefficients overall. The following forms the outline of the dissertation.

The chapter 1 discuss regarding the importance of thermal management of heatsink and microprocessors, as well as research conducted based on the topic related to it. It relates to the literature survey based on thermal management of electronic components as well as infrared thermographic study to know about the thermal profiles. At the end, an objective of the dissertation is highlighted.

The chapter 2 discuss regarding the conditions and stages used for both simulation and experimental purpose.

The chapter 3 discuss regarding simulation method. It describes the simulation model, meshing (grid generation), governing equation and boundary conditions used for simulation purpose. It also shows the simulation results obtained through ANSYS software.

The chapter 4 discuss regarding experimental method. The experimental method describes the methodology, means how thermal image camera can be used for obtaining thermal profiles and noting down the temperature. It also describes the experimental results.

An analysis between simulation and experimental method has been produced. It also shows the pattern of air flow obtained through simulation as a part of discussion.

The chapter 6 represent the conclusion of the dissertation. A proposed model has also been discussed as part of future scope.

1.2. Aim of the research

In this research we want to focus mainly on the following points:

- In this work, thermal analysis for the microprocessor is done using a simulation method and an experimental method.
- The simulation method is done by adding heat flux at the base surface of microprocessor at specific increments with respect to time and noting down the temperature of the microprocessor.
- The experimental method is done by using Fluke Ti 450 thermal image camera, the camera is used for taking pictures (thermal profiles) and observing the temperature of microprocessors with respect to time same as that of the simulation method.
- Both the simulation and experimental methods are done under two conditions: no load and load.
- In the end, an analysis of both the results of the simulation and experimental method is done.
- Also, we will try to find out a method for reducing the temperature of the microprocessor to an extent as a future scope.

CHAPTER 2

THEORETICAL STUDY

The simulation and experimental analysis for heat sink and microprocessors of CPU under no load and load conditions with respect to time was conducted in four stages: 1) With heat sink and fan on; 2) With heat sink, fan on and in between placing an obstacle; 3) With heat sink and fan off; and finally, by 4) removing heat sink (on microprocessor) and fan off. Duration of the experiment was 2 hours for each condition. Ambient temperature was around 29^0C - 30^0C.

Below figure shows the block diagram for each condition

1) Experiment with heat sink and fan on condition

Analysis have been conducted for the experiment with heat sink 1 and fan on condition by both numerical and experimental method. Ambient temperature was 29^0C. It has been described in Figure 2.1

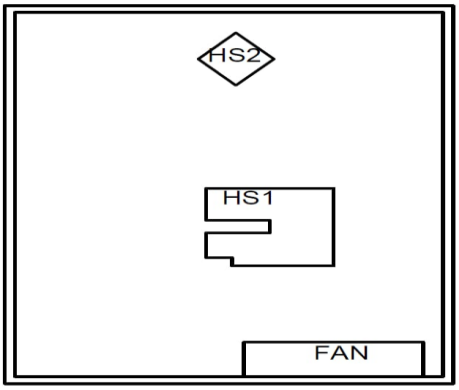

Fig. 2.1. Schematic diagram of the experiment with heat sink and fan on condition

2) Experiment with heat sink, fan on and in between placing an obstacle

Analysis have been conducted for the experiment with heat sink 1, fan on and in between placing an obstacle condition by both numerical and experimental method. Obstacle used for the experiment is book of dimension 105mm×80mm×2mm book was resting on its longest side of

105mm length. The obstacle was placed 24mm from the fan and was in between heat sink 1. Ambient temperature was 30^0C. It has been described in Figure 2.2

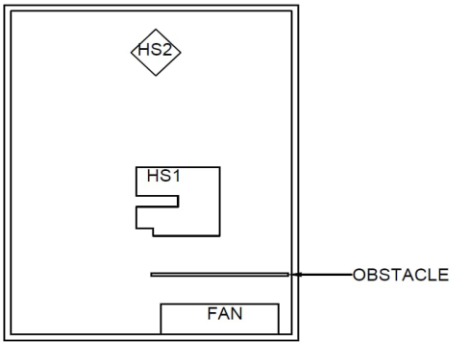

Fig. 2.2. Schematic diagram of the experiment with heat sink, fan on and in between placing an obstacle condition

3) Experiment with heat sink and fan off condition

Analysis have been conducted for the experiment with heat sink 1 and fan off condition by both numerical and experimental method. Ambient temperature was 29^0C. It has been described in Figure 2.3

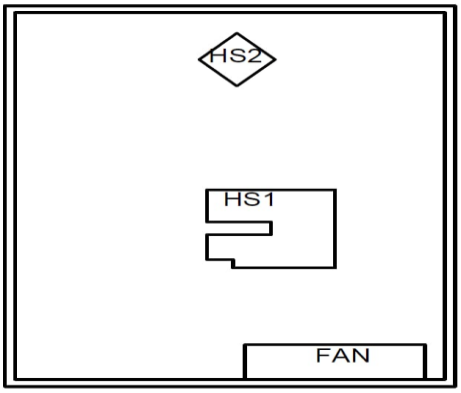

Fig. 2.3. Schematic diagram of the experiment with heat sink and fan off condition

4) Experiment with heat sink 1 removed, fan off and temperature measurements taken on microprocessor

Analysis have been conducted for the experiment with microprocessor (heatsink 1 removed) and fan off condition by both numerical and experimental method. Ambient temperature was 29^0C. It has been described in Figure 2.4

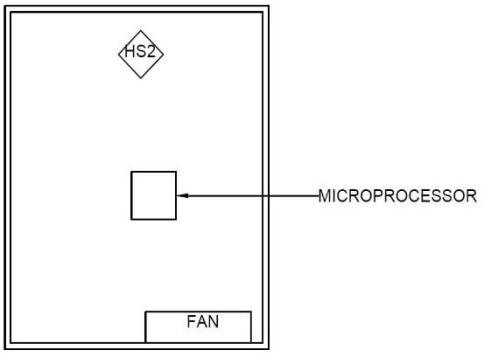

Fig. 2.4. Schematic diagram of the experiment with microprocessor and fan off condition

CHAPTER 3

SIMULATION METHOD

3.1. Modelling

The software used for entire numerical process is ANSYS 2023 R1 STUDENT version. The modelling is done by ANSYS Spaceclaim modeler which give ease of access in constructing the model, saving time compared to ANSYS Design modeler. The whole CPU model is of the dimension 265×215×110 mm. The microprocessor dimension is 37.5×37.5×2 mm. Aluminium material for both heat sinks and Silicon material for microprocessor was adopted. The dimensions for the model have been taken from the CPU model HP COMPAQ ELITE 8300 SFF. The modelling has been described in Figure 3.1.

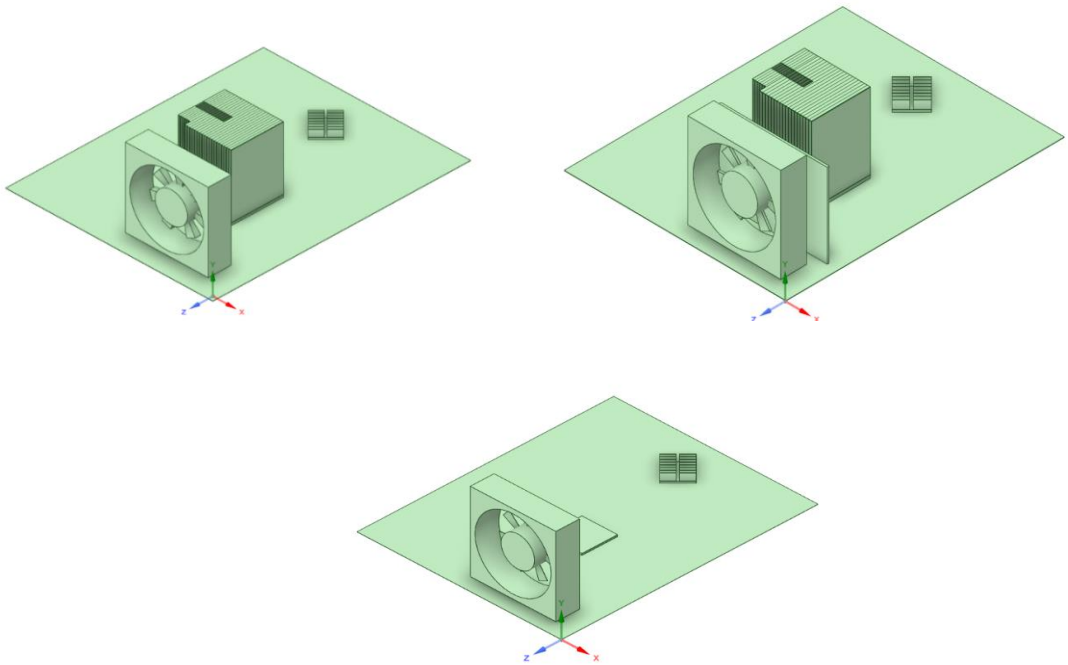

Fig. 3.1. ANSYS model designed for simulation purpose

3.2. Grid generation – Meshing

The model generated from ANSYS Spaceclaim is imported in to ANSYS meshing. The element size was set to 0.015m. The skewness was in the range 0 – 0.8 for the entire model which indicates mesh quality was acceptable. Non uniform mesh has been inserted into the model because shape of the model is different. Adaptive meshing option has been selected for generating non uniform meshing. Meshing is done on the boundary of the model not inside the model. Other setting of the mesh was set to default.

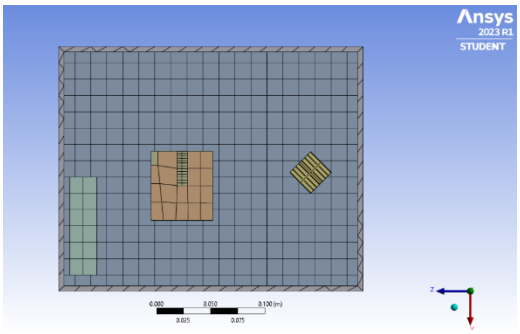

Fig. 3.2a

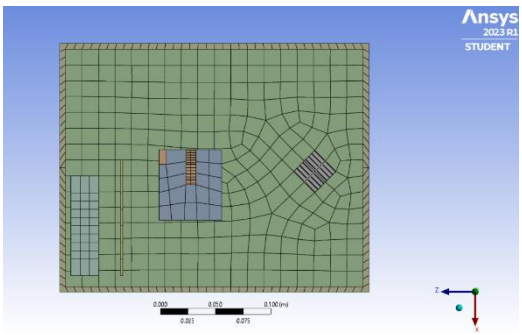

Fig. 3.2b

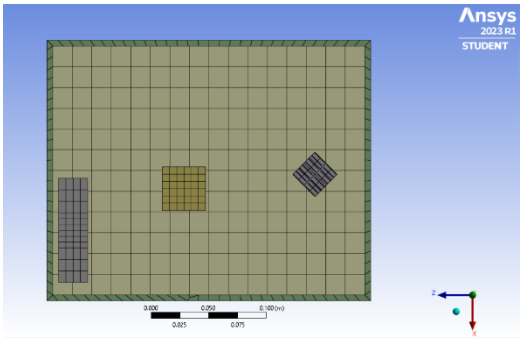

Fig. 3.2c

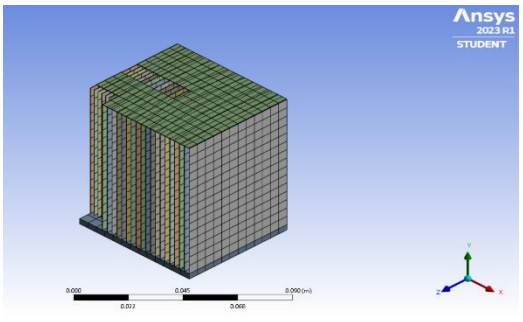

Fig. 3.2d

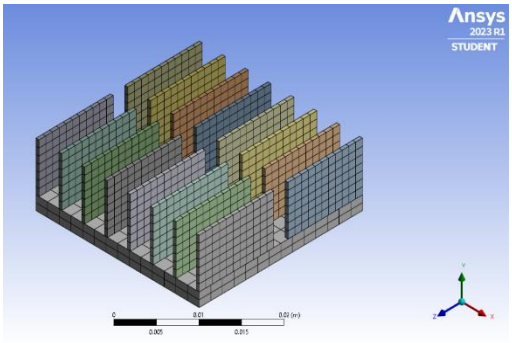

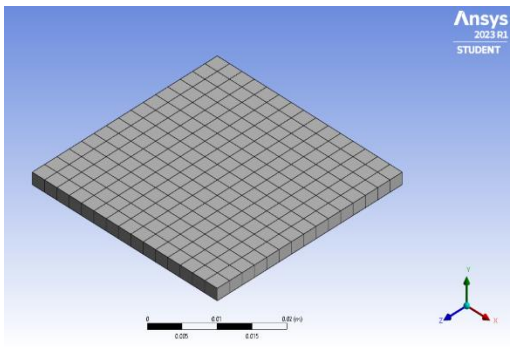

Fig. 3.2e **Fig. 3.2f**

Fig. 3.2. The mesh generated has been shown for different conditions and components

3.3. Governing Equations

Continuity Equation:

$$\frac{\partial}{\partial x_i}(\rho u_i) = 0 \tag{1}$$

Momentum Equation:

$$\frac{\partial}{\partial x_j}(\rho u_i u_j) = -\frac{\partial p}{\partial x_i} + \frac{\partial \tau_{ij}}{\partial x_j} + \rho g_i \tag{2}$$

where shear stress components, $\tau_{ij} = \left[\mu\left(\frac{\partial u_i}{\partial x_j} + \frac{\partial u_j}{\partial x_i}\right)\right] - \frac{2}{3}\mu\frac{\partial u_i}{\partial x_i}\delta_{ij}$ (3)

From the mass conservation equation,

Mass cannot be created or destroyed within the control volume.

Rate of mass accumulation within the control volume = Net rate of mass flow into the control volume

Rate of mass accumulation within the control volume = $\frac{\partial}{\partial t}(\rho \Delta V)$

Net rate of mass flow into the control volume = Mass flow rate entering the control volume – Mass flow rate exiting the control volume

i.e., = Mass flux at the inlet – Mass flux at the outlet

$= \rho 1 u 1 n 1 - \rho 2 u 2 n 2$

Net rate of mass flow into the control volume = $(\rho 1u1n1)A1 - (\rho 2u2n2)A2$

Where A is the cross-sectional area and n1 and n2 are the unit normal vectors to the control surface at the inlet and outlet,

Now equating the rate of mass accumulation within the control volume and net rate of mass flow into the control volume,

$\frac{\partial}{\partial t}(\rho \Delta V) = (\rho 1u1n1)A1 - (\rho 2u2n2)A2$

Dividing through by ΔV and taking the limit as ΔV approaches zero

$$\frac{\partial \rho}{\partial t} + \frac{\partial}{\partial x_i}(\rho u_i) = 0 \qquad (4)$$

From Navier Stokes Equation, momentum conservation equation is as follows:

General form of conservation of momentum equation,

$$\frac{\partial}{\partial t}(\rho ui) + \frac{\partial}{\partial x}(\rho uiuj) = \frac{\partial}{\partial x}\tau + \rho f$$

Convective term, $\frac{\partial}{\partial t}(\rho ui)$ represents the change in momentum due to the acceleration of fluid particles in time.

By product rule, $\frac{\partial}{\partial t}(\rho ui) = \rho \frac{\partial ui}{\partial t} + ui \frac{\partial \rho}{\partial t}$

Convective flux term, $\frac{\partial}{\partial x}(\rho uiuj)$ relates to advection of momentum in space.

$$\frac{\partial}{\partial x}(\rho uiuj) = \left(\frac{\partial}{\partial x}\rho ui\right)uj + \rho\left(\frac{\partial}{\partial x}ui\right)uj + \rho ui\frac{\partial}{\partial x}uj$$

Diffusive term $\mu \frac{\partial}{\partial x}\left(\frac{\partial ui}{\partial x}\right)$ means viscous forces acting on the fluid

Expanding the diffusive term,

$$\mu \frac{\partial}{\partial x}\left(\frac{\partial ui}{\partial x}\right) = \mu \frac{\partial}{\partial x}\left(\frac{\partial ui}{\partial x}\right)$$

External force represents any force acting on the fluid – Fi

Combining all terms,

$$\frac{\partial}{\partial t}(\rho u_i) + \frac{\partial}{\partial x_j}(\rho u_j u_i) = -\frac{\partial p}{\partial x_i} + \frac{\partial}{\partial x_j}\left(\mu \frac{\partial u_i}{\partial x_j}\right) + Fi \quad (5)$$

where, ρ is density, u_i is velocity, p is pressure, μ is dynamic viscosity and F_i is external force.

Energy conservation equation is described by,

From general conservation of energy equation

$$\frac{\partial}{\partial t}(\rho U) + \frac{\partial}{\partial x}(\rho U u) = \frac{\partial}{\partial x}\left(k \frac{\partial T}{\partial x}\right) + \emptyset$$

Rate of change of total energy within a control volume is equal to the net rate of energy entering or leaving the control volume.

Expanding the convective term using product rule

$$\frac{\partial}{\partial t}(\rho U) + \frac{\partial}{\partial x}(\rho U u) = \frac{\partial}{\partial t}(\rho U) + v\frac{\partial}{\partial x}(\rho U) + \rho U \frac{\partial}{\partial x} u$$

First law of thermodynamics

$$\frac{\partial}{\partial t}(\rho U) = \frac{\partial}{\partial t}(\rho c T)$$

U – Internal Energy, T – Temperature, ρcT - Time derivative of ρU w.r.t time

Substitute the expanded convective and conductive term into conservation of energy equation,

$$\frac{\partial}{\partial t}(\rho c T) + v\frac{\partial}{\partial x}(\rho U) + \rho U \frac{\partial}{\partial x} u = \frac{\partial}{\partial x}\left(K \frac{\partial T}{\partial x}\right) + \emptyset$$

Expand the term $v\frac{\partial}{\partial x}(\rho U)$ using product rule,

$$u\frac{\partial}{\partial x}(\rho U) = u\left(\rho \frac{\partial}{\partial x} U\right) + \rho U \frac{\partial}{\partial x} u$$

Rearranging,

$$\frac{\partial}{\partial t}(\rho c T) + u\left(\rho \frac{\partial}{\partial x} U\right) + \rho U \frac{\partial}{\partial x} u = \frac{\partial}{\partial x}\left(k \frac{\partial}{\partial x} T\right) + \emptyset$$

Applying continuity equation,

$$\frac{\partial}{\partial x}(\rho u) = 0$$

(To eliminate $\left(\rho \frac{\partial}{\partial x} Uu\right)$)

$$\frac{\partial}{\partial t}(\rho cT) + \rho U \frac{\partial}{\partial x} u = \frac{\partial}{\partial x}\left(k\left(\frac{\partial T}{\partial x}\right)\right) + \emptyset$$

The term ρU represents total energy per unit volume – E

$$\frac{\partial}{\partial t}(\rho cT) + \rho E \frac{\partial}{\partial x} u = \frac{\partial}{\partial x}\left(k \frac{\partial T}{\partial x}\right) + \emptyset$$

$$\rho c_p \left[\left(\frac{\partial T}{\partial t}\right) + u_i \left(\frac{\partial T}{\partial x_i}\right)\right] = \frac{\partial}{\partial x_i}\left(K \frac{\partial T}{\partial x_i}\right) + \emptyset \qquad (6)$$

where, T is temperature, c_p is specific heat capacity, k is thermal conductivity, φ is the rate of internal heat generation per unit volume.

The Navier Stokes Equation (5) helps in understanding the distribution of air velocities and pressures which can guide the design of heat sink and fan. Forces influences the air flow pattern and determine how effectively heat is dissipated from the microprocessor. Energy equation (6) is an Unsteady Temperature equation, where temperature is varied with respect to time. The term φ denotes the heat generation within the heat source. In the ANSYS software, Finite Element Method has been taken for solving which is inbuilt in the software. The energy equation helps in understanding how heat is transferred from microprocessor to surrounding environment and heat sink.

3.4. Boundary Conditions

According to Newton's Law of Cooling convective heat transfer,

$$Q_{conv} = hA(Tb - Ta) \qquad (7)$$

Based on the assumption heat flux of microprocessor is varied from 50W/cm^2 to 110W/cm^2 with respect to load [29], following input has been provided:

A) With heat sink and fan on condition

A1) Heat Sink 1

i) No load – Constant heat flux of 50 W/cm^2 was applied.

ii) Load – Heat flux starting from 50 W/cm^2 and with an increment of 0.5 W/cm^2 at every five minutes up to a duration of 120 minutes was applied.

A2) Heat Sink 2

i) No load – Constant heat flux of 50 W/cm^2 was applied.

ii) Load – Heat flux starting from 50 W/cm^2 and with an increment of 0.5 W/cm^2 at every five minutes up to a duration of 120 minutes was applied.

CPU fan velocity was set to v = 11m/s (inlet velocity and outlet pressure). This was the fluid (air) condition on the CPU chassis.

B) With heat sink and fan on condition, placing an obstacle in between heatsink 1 and fan.

B1) Heat Sink 1

i) No load – Heat flux starting from 50 W/cm^2 and with an increment of 0.2 W/cm^2 at every five minutes up to a duration of 120 minutes was applied.

ii) Load - Heat flux starting from 50 W/cm^2 and with an increment of 0.8 W/cm^2 at every five minutes up to a duration of 120 minutes was applied.

B2) Heat Sink 2

i) No load - Heat flux starting from 50 W/cm^2 and with an increment of 0.5 W/cm^2 at every five minutes up to a duration of 120 minutes was applied.

ii) Load - Heat flux starting from 50 W/cm^2 and with an increment of 1 W/cm^2 at every five minutes up to a duration of 120 minutes was applied.

CPU fan velocity was set to v = 11m/s (inlet velocity and outlet pressure). This was the fluid (air) condition on the CPU chassis.

C) With heat sink and fan off condition

C1) Heat Sink 1

i) No load - Heat flux starting from 50 W/cm^2 and with an increment of 1.2 W/cm^2 at every five minutes up to a duration of 120 minutes was applied.

ii) Load - Heat flux starting from 50 W/cm^2 and with an increment of 1.5 W/cm^2 at every five minutes up to a duration of 120 minutes was applied.

C2) Heat Sink 2

i) No load - Heat flux starting from 50 W/cm^2 and with an increment of 1.5 W/cm^2 at every five minutes up to a duration of 120 minutes was applied.

ii) Load - Heat flux starting from 50 W/cm^2 and with an increment of 1.8 W/cm^2 at every five minutes up to a duration of 120 minutes was applied.

CPU fan velocity was set to v = 0 m/s and pressure was set with respect to atmospheric condition, P = 101325Pa (inlet pressure and outlet pressure). This was the fluid (air) condition on the CPU chassis.

D) Microprocessor – Fan off condition (Heat Sink 1 removed)

i) No load - Heat flux starting from 50 W/cm^2 and with an increment of 1.8 W/cm^2 at every five minutes up to a duration of 120 minutes was applied.

ii) Load - Heat flux starting from 50 W/cm^2 and with an increment of 2.1 W/cm^2 at every five minutes up to a duration of 120 minutes was applied.

CPU fan velocity was set to v = 0 m/s and pressure was set with respect to atmospheric condition, P = 101325Pa (inlet pressure and outlet pressure). This was the fluid (air) condition on the CPU chassis.

Schematic model of the project for boundary conditions has been shown in Figure 3.3

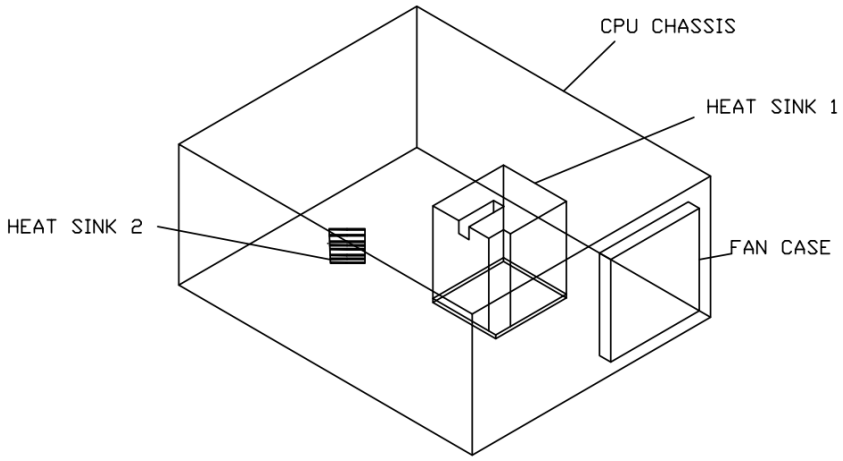

Fig. 3.3. Schematic of CPU model for the research

3.5. Simulation results

From the Figure 3.4. shows temperature distribution or thermal profile of heat sink 1, heat sink 2 and for microprocessor are shown separately. Dark blue indicates the lowest temperature and Red indicates the highest temperature. For heat sink 1 and heat sink 2 top surfaces has the lowest temperature, from there temperature increases to bottom surface. In the case of microprocessor temperature contour indicates that temperature close to maximum temperature is on the central portion of the surface, and at the surface closer to the boundary, temperature is less than that of temperature at central portion of surface. Maximum temperature for the microprocessor is seen at bottom surface.

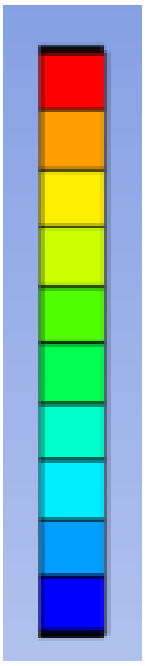

Fig.3.4a

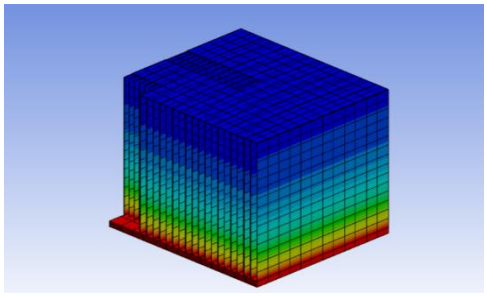

Fig.3.4b

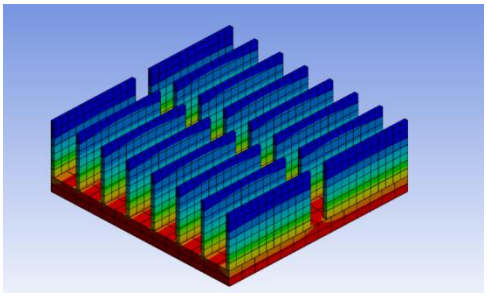

Fig.3.4c

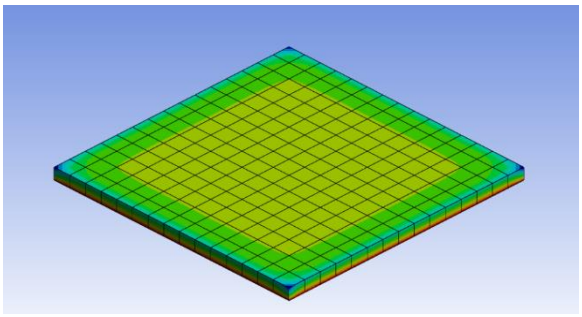

Fig.3.4d

Fig.3.4a. Temperature contour, **Fig.3.4b** Heat sink 1 (HS1), **Fig.3.4c** Heat sink 2 (HS2), **Fig.3.4d** Microprocessor

1(a): Under no load condition; Fan on, with heat sink 1; Ambient temperature 29^{0}C

The following Table 3.1. show the results for heat sink 1 under no load – fan on condition, the ambient temperature was 29^{0}C. Highest temperature at 120th minute observed was 30.1^{0}C.

Table 3.1. Temperature measurements for HS1 under no load and fan on condition

TIME (minute)	T1(Celsius)	T2(Celsius)	T3(Celsius)	Tc(Celsius)
0	30.1	30.1	30.1	30.1
5	29.8	29.8	29.8	29.8
10	29.6	29.6	29.6	29.6
15	30.1	30.1	30.1	30.1
20	29.9	29.9	29.9	29.9
25	29.7	29.7	29.7	29.7
30	29.8	29.8	29.8	29.8
35	29.7	29.7	29.7	29.7
40	29.9	29.9	29.9	29.9
45	30.1	30.1	30.1	30.1

50	29.9	29.9	29.9	29.9
55	29.7	29.7	29.7	29.7
60	29.8	29.8	29.8	29.8
65	29.7	29.7	29.7	29.7
70	29.9	29.9	29.9	29.9
75	29.6	29.6	29.6	29.6
80	29.8	29.8	29.8	29.8
85	29.9	29.9	29.9	29.9
90	30	30	30	30
95	29.9	29.9	29.9	29.9
100	29.8	29.8	29.8	29.8
105	29.9	29.9	29.9	29.9
110	29.6	29.6	29.6	29.6
115	29.1	29.1	29.1	29.1
120	30.1	30.1	30.1	30.1

1(b): Under no load condition; Fan on, with heat sink 2; Ambient temperature 29^0C

The following Table 3.2 show the results for heat sink 2 under no load – fan on condition, the ambient temperature was 29^0C. Highest temperature at 120^{th} minute observed was 31.8^0C.

Table 3.2 Temperature measurements for HS2 under no load and fan on condition

TIME (minute)	T1(Celsius)	T2(Celsius)	T3(Celsius)	Tc (Celsius)
0	30.6	30.6	30.6	30.6
5	30.8	30.8	30.8	30.8
10	30.6	30.6	30.6	30.6
15	30.9	30.9	30.9	30.9
20	30.6	30.6	30.6	30.6
25	30.8	30.8	30.8	30.8
30	30.6	30.6	30.6	30.6
35	30.8	30.8	30.8	30.8
40	30.7	30.7	30.7	30.7

45	30.9	30.9	30.9	30.9
50	30.4	30.4	30.4	30.4
55	30.6	30.6	30.6	30.6
60	30.7	30.7	30.7	30.7
65	30.6	30.6	30.6	30.6
70	30.7	30.7	30.7	30.7
75	30.9	30.9	30.9	30.9
80	30.7	30.7	30.7	30.7
85	31.4	31.4	31.4	31.4
90	31.6	31.6	31.6	31.6
95	31.5	31.5	31.5	31.5
100	31.8	31.8	31.8	31.8
105	31.7	31.7	31.7	31.7
110	31.6	31.6	31.6	31.6
115	31.9	31.9	31.9	31.9
120	31.8	31.8	31.8	31.8

Figure 3.5. shows the graph for median temperature analysis under no load – fan on condition for heat sink 1 and heat sink 2.

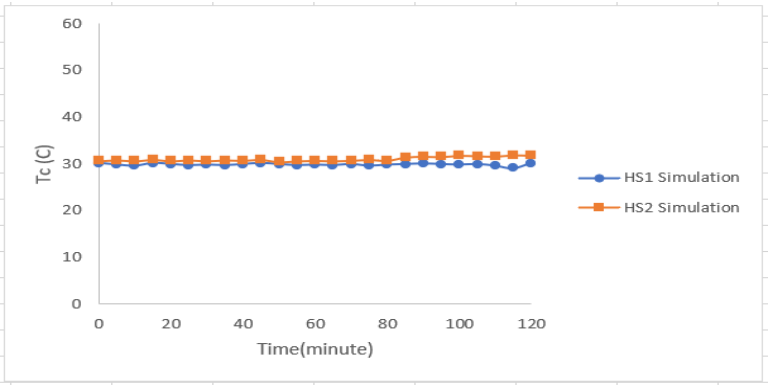

Fig.3.5. Graph shows the median temperature measurements for HS1 and HS2 under no load and fan on condition

Figure 3.6 shows the thermal profile obtained through simulation under no load – fan on condition at different time period.

t = 60 minute

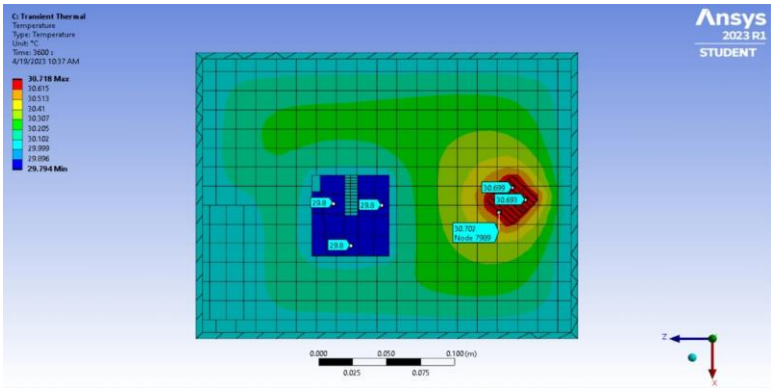

t = 120 minute

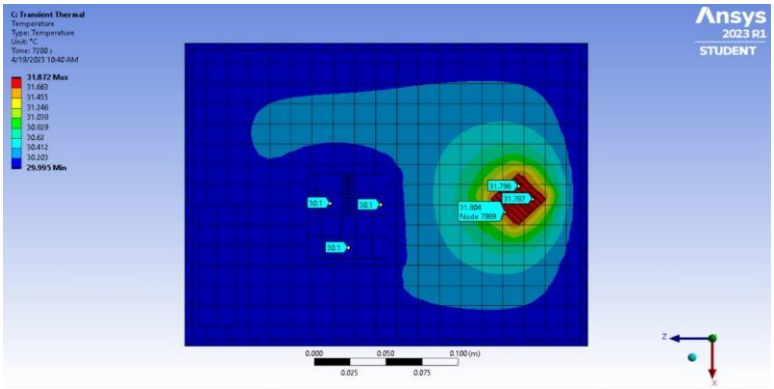

Fig. 3.6. Temperature contours obtained through simulation at different time periods

1(c): Under load condition; Fan on, with heat sink 1; Ambient temperature 29^{0}C

The following Table 3.3 show the results for heat sink 1 under load – fan on condition, the ambient temperature was 29^{0}C. Highest temperature at 120th minute observed was 45^{0}C.

Table 3.3. Temperature measurements for HS1 under load and fan on condition

TIME (minute)	T1(Celsius)	T2(Celsius)	T3(Celsius)	Tc (Celsius)
0	30.3	30.3	30.3	30.3
5	31.4	31.4	31.4	31.4
10	31.7	31.7	31.7	31.7
15	32.3	32.3	32.3	32.3
20	32.9	32.9	32.9	32.9
25	33.8	33.8	33.8	33.8

30	34.2	34.2	34.2	34.2
35	34.6	34.6	34.6	34.6
40	35.4	35.4	35.4	35.4
45	35.9	35.9	35.9	35.9
50	36.5	36.5	36.5	36.5
55	37.9	37.9	37.9	37.9
60	39.1	39.1	39.1	39.1
65	39.4	39.4	39.4	39.4
70	39.5	39.5	39.5	39.5
75	39.7	39.7	39.7	39.7
80	40.3	40.3	40.3	40.3
85	40.7	40.7	40.7	40.7
90	41	41	41	41
95	41.7	41.7	41.7	41.7
100	42.3	42.3	42.3	42.3
105	42.8	42.8	42.8	42.8
110	43.4	43.4	43.4	43.4
115	43.7	43.7	43.7	43.7
120	45	45	45	45

1(d): Under load condition; Fan on, with heat sink 2; Ambient temperature 29^0C

The following Table 3.4 show the results for heat sink 2 under load – fan on condition, the ambient temperature was 29^0C. Highest temperature at 120^{th} minute observed was 48.8^0C.

Table 3.4. Temperature measurements for HS2 under load and fan on condition

TIME (minute)	T1(Celsius)	T2(Celsius)	T3(Celsius)	Tc(Celsius)
0	29.6	29.6	29.6	29.6
5	30.6	30.6	30.6	30.6
10	31.4	31.4	31.4	31.4
15	32.8	32.8	32.8	32.8
20	33.5	33.5	33.5	33.5

25	34.3	34.3	34.3	34.3
30	35.6	35.6	35.6	35.6
35	36.4	36.4	36.4	36.4
40	37.3	37.3	37.3	37.3
45	38.3	38.3	38.3	38.3
50	39.4	39.4	39.4	39.4
55	40.5	40.5	40.5	40.5
60	41.4	41.3	41.4	41.4
65	42.3	42.3	42.3	42.3
70	42.7	42.7	42.7	42.7
75	43.1	43.1	43.1	43.1
80	43.8	43.8	43.8	43.8
85	44.6	44.6	44.6	44.6
90	45.7	45.6	45.8	45.7
95	45.8	45.8	45.8	45.8
100	46.3	46.3	46.3	46.3
105	46.9	46.9	46.9	46.9
110	47.4	47.4	47.4	47.4
115	47.9	47.9	47.9	47.9
120	48.8	48.7	48.9	48.8

Figure 3.7 shows the graph for median temperature analysis under load – fan on condition for heat sink 1 and heat sink 2 respectively

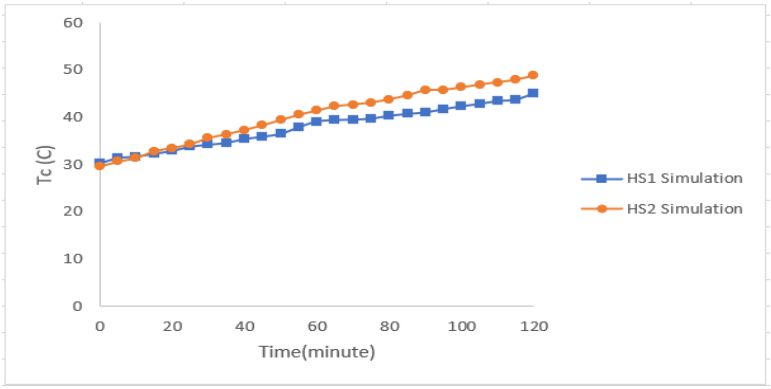

Fig. 3.7. Graph shows the median temperature measurements for HS1 and HS2 under load and fan on condition

Figure 3.8. shows the thermal profile obtained through simulation under load – fan on condition at different time period in the CPU chassis.

t = 60 minute

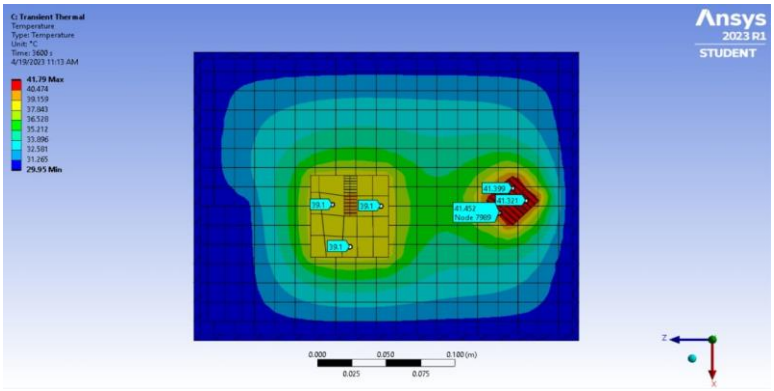

t = 120 minute

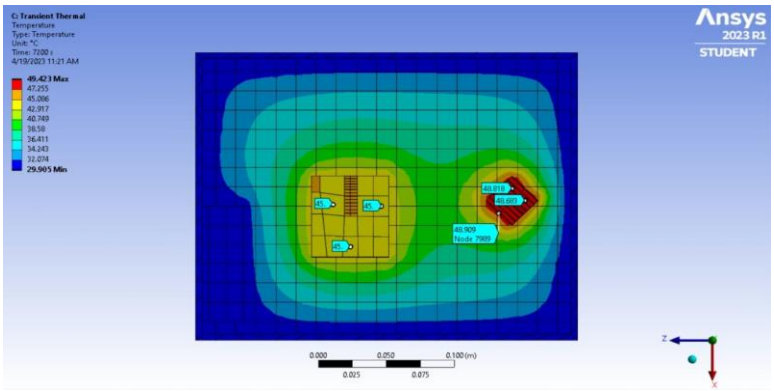

Fig. 3.8. Temperature contours obtained through simulation at different time periods

2: With obstacle – Obstacle used for the experiment is book of dimension 105mm×80mm×2mm book was resting on its longest side of 105mm length. The obstacle was placed 24mm from the fan and was in between heat sink 1.

2(a): Under no load condition; With obstacle, Fan on, with heat sink 1; Ambient temperature 29^0C

Table 3.5. show the results for heat sink 1 under no load – fan off with obstacle condition, the ambient temperature was 30^0C. Highest temperature at 120^{th} minute observed was 34.3^0C.

Table 3.5. Temperature measurements for HS1 under no load, fan on and by placing an obstacle condition

TIME (minute)	T1(Celsius)	T2(Celsius)	T3(Celsius)	Tc (Celsius)
0	30.9	30.9	30.9	30.9
5	31.1	31.1	31.1	31.1
10	31.3	31.3	31.3	31.3
15	31.5	31.5	31.5	31.5
20	31.9	31.9	31.9	31.9
25	32.4	32.4	32.4	32.4
30	32.8	32.8	32.8	32.8
35	32.5	32.5	32.5	32.5
40	32.3	32.3	32.3	32.3
45	32.6	32.6	32.6	32.6
50	32.5	32.5	32.5	32.5
55	32.6	32.6	32.6	32.6
60	33	33	33	33
65	32.9	32.9	32.9	32.9
70	33.4	33.4	33.4	33.4
75	33.6	33.6	33.6	33.6
80	33.8	33.8	33.8	33.8
85	33.7	33.7	33.7	33.7
90	34.2	34.2	34.2	34.2
95	34.4	34.4	34.4	34.4
100	34.3	34.3	34.3	34.3

105	34.5	34.5	34.5	34.5
110	34.2	34.2	34.2	34.2
115	34.4	34.4	34.4	34.4
120	34.3	34.3	34.3	34.3

2(b): Under no load condition; With obstacle, Fan on, with heat sink 2; Ambient temperature 29^0C

Table 3.6 show the results for heat sink 2 under no load – fan off with obstacle condition, the ambient temperature was 29^0C. Highest temperature at 120^{th} minute observed was 35.3^0C.

Table 3.6. Temperature measurements for HS2 under no load, fan on and by placing an obstacle condition

TIME (minute)	T1(Celsius)	T2(Celsius)	T3(Celsius)	Tc (Celsius)
0	30.9	30.9	30.9	30.9
5	31.2	31.2	31.2	31.2
10	31.4	31.4	31.4	31.4
15	31.5	31.5	31.5	31.5
20	31.8	31.8	31.8	31.8
25	31.9	31.9	31.9	31.9
30	32	32	32	32
35	32.2	32.2	32.2	32.2
40	32.7	32.7	32.7	32.7
45	33.4	33.4	33.4	33.4
50	33.9	33.9	33.9	33.9
55	34.7	34.7	34.7	34.7
60	35.9	35.9	35.9	35.9
65	35.4	35.4	35.4	35.4
70	35.6	35.6	35.6	35.6
75	35.3	35.3	35.3	35.3
80	35.6	35.6	35.6	35.6
85	35.4	35.4	35.4	35.4
90	35.9	35.9	35.9	35.9

95	35.6	35.6	35.6	35.6
100	35.4	35.4	35.4	35.4
105	35.2	35.2	35.2	35.2
110	35.5	35.5	35.5	35.5
115	35.2	35.2	35.2	35.2
120	35.3	35.3	35.3	35.3

Figure 3.9 shows the graph for median temperature analysis under no load – fan on with obstacle condition for heat sink 1 and heat sink 2.

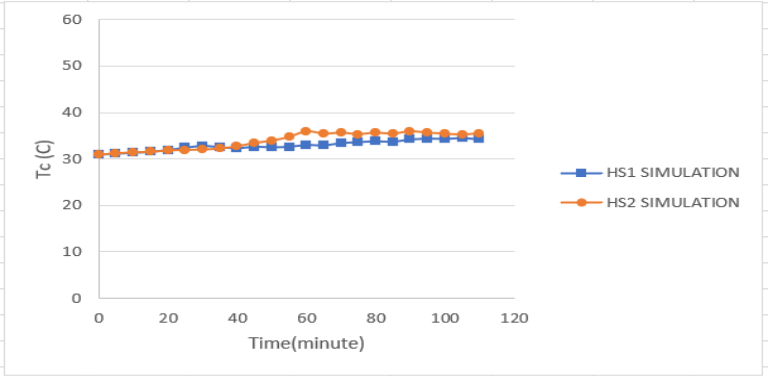

Fig. 3.9. Graph shows the median temperature measurements for HS1 and HS2 under no load and fan on with obstacle condition

t = 60 minute

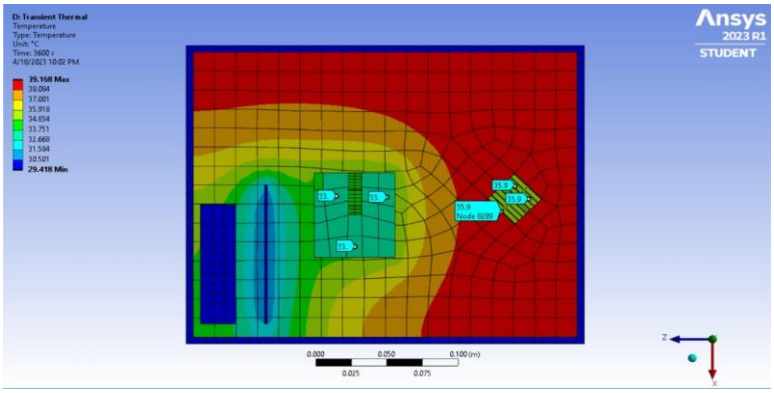

t = 120 minute

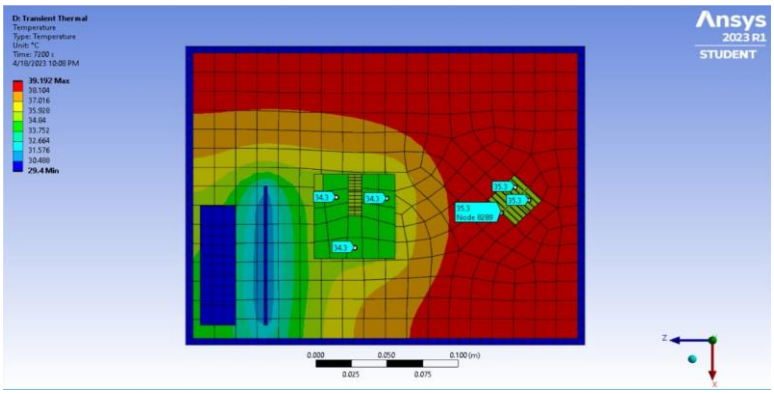

Fig. 3.10. Temperature contours obtained through simulation at different time periods

2(c): Under load condition; With obstacle, Fan on, with heat sink 1; Ambient temperature 29^{0}C

The following Table 3.7 show the results for heat sink 1 under load – fan off with obstacle condition, the ambient temperature was 29^{0}C. Highest temperature at 120th minute observed was 48.7^{0}C.

Table 3.7. Temperature measurements for HS1 under load, fan on and by placing an obstacle condition

TIME (minute)	T1(Celsius)	T2(Celsius)	T3(Celsius)	Tc (Celsius)
0	29.8	29.8	29.8	29.8
5	30.7	30.7	30.7	30.7
10	31.8	31.8	31.8	31.8
15	32.8	32.8	32.8	32.8
20	33.6	33.6	33.6	33.6
25	34	34	34	34
30	34.8	34.8	34.8	34.8
35	34.9	34.9	34.9	34.9
40	35.2	35.2	35.2	35.2
45	35.9	35.9	35.9	35.9
50	36.3	36.3	36.3	36.3
55	36.8	36.8	36.8	36.8
60	37.4	37.4	37.4	37.4

65	38.4	38.4	38.4	38.4
70	39.4	39.4	39.4	39.4
75	40.8	40.8	40.8	40.8
80	41.7	41.7	41.7	41.7
85	42.8	42.8	42.8	42.8
90	43.8	43.8	43.8	43.8
95	44.7	44.7	44.7	44.7
100	44.9	44.9	44.9	44.9
105	45.4	45.4	45.4	45.4
110	46.9	46.9	46.9	46.9
115	47.6	47.6	47.6	47.6
120	48.7	48.7	48.7	48.7

2(d): Under load condition; With obstacle, Fan on, with heat sink 2; Ambient temperature 29^0C

The following Table 3.8 show the results for heat sink 2 under load – fan off with obstacle condition, the ambient temperature was 29^0C. Highest temperature at 120^{th} minute observed was 50.9^0C.

Table 3.8. Temperature measurements for HS2 under load, fan on and by placing an obstacle condition

TIME (minute)	T1(Celsius)	T2(Celsius)	T3(Celsius)	Tc (Celsius)
0	30.1	30.1	30.1	30.1
5	30.7	30.7	30.7	30.7
10	31.7	31.7	31.7	31.7
15	32.6	32.6	32.6	32.6
20	33.8	33.8	33.8	33.8
25	34.9	34.9	34.9	34.9
30	36.4	36.4	36.4	36.4
35	36.5	36.5	36.5	36.5
40	36.7	36.7	36.7	36.7
45	37.7	37.7	37.7	37.7
50	38.3	38.3	38.3	38.3

55	39.4	39.4	39.4	39.4
60	39.9	39.9	39.9	39.9
65	40.4	40.4	40.4	40.4
70	41.4	41.4	41.4	41.4
75	42.6	42.6	42.6	42.6
80	43.5	43.5	43.5	43.5
85	43.9	43.9	43.9	43.9
90	45.1	45.1	45.1	45.1
95	45.5	45.5	45.5	45.5
100	46.7	46.7	46.7	46.7
105	47.9	47.9	47.9	47.9
110	48.9	48.9	48.9	48.9
115	49.9	49.9	49.9	49.9
120	50.9	50.9	50.9	50.9

Figure 3.11 shows the graph for median temperature analysis under load – fan on condition for heat sink 1 and heat sink 2 respectively

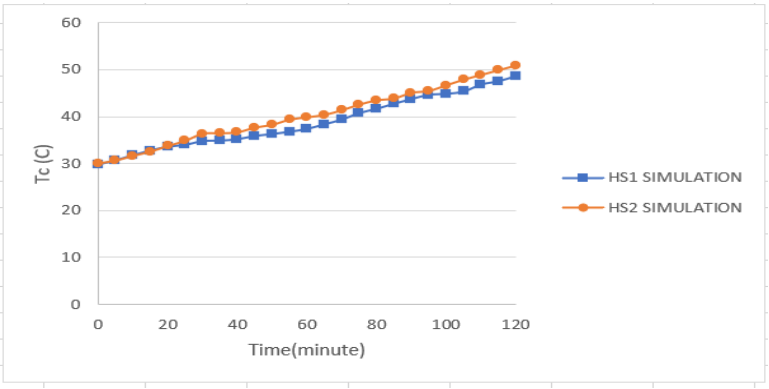

Fig. 3.11. Graph shows the median temperature measurements for HS1 and HS2 under load and fan on with obstacle condition

t = 60 minute

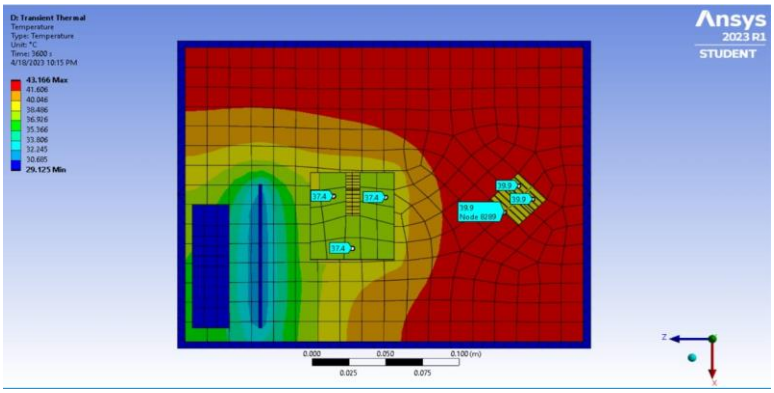

t = 120 minute

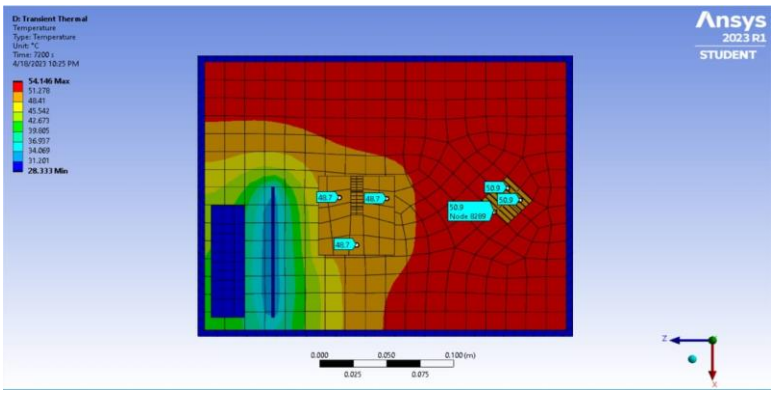

Fig. 3.12. Temperature contours obtained through simulation at different time periods

3(a): Under no load condition; Fan off, with heat sink 1; Ambient temperature 29^{0}C

Table 3.9 show the results for heat sink 1 under no load – fan off condition, the ambient temperature was 29^{0}C. Highest temperature at 120th minute observed was 41.2^{0}C.

Table 3.9. Temperature measurements for HS1 under no load and fan off condition

TIME (minute)	T1(Celsius)	T2(Celsius)	T3(Celsius)	Tc (Celsius)
0	29.7	29.7	29.7	29.7
5	30.6	30.6	30.6	30.6
10	30.8	30.8	30.8	30.8
15	31.8	31.8	31.8	31.8
20	32.5	32.5	32.5	32.5
25	32.7	32.7	32.7	32.7

30	34	34	34	34
35	33.9	33.9	33.9	33.9
40	34.6	34.6	34.6	34.6
45	34.9	34.9	34.9	34.9
50	35.5	35.5	35.5	35.5
55	35.9	35.9	35.9	35.9
60	36.1	36.1	36.1	36.1
65	36.3	36.3	36.3	36.3
70	36.4	36.4	36.4	36.4
75	36.7	36.7	36.7	36.7
80	36.9	36.9	36.9	36.9
85	37.3	37.3	37.3	37.3
90	37.8	37.8	37.8	37.8
95	38	38	38	38
100	38.2	38.2	38.2	38.2
105	38.6	38.6	38.6	38.6
110	38.9	38.9	38.9	38.9
115	40.5	40.5	40.5	40.5
120	41.2	41.2	41.2	41.2

3(b): Under no load condition; Fan off, with heat sink 2; Ambient temperature 29^0C

Table 3.10 show the results for heat sink 2 under no load – fan off condition, the ambient temperature was 29^0C. Highest temperature at 120^{th} minute observed was 42.9^0C.

Table 3.10. Temperature measurements for HS2 under no load and fan off condition

TIME (minute)	T1(Celsius)	T2(Celsius)	T3(Celsius)	Tc (Celsius)
0	30.6	30.6	30.6	30.6
5	30.9	30.9	30.9	30.9
10	31.5	31.5	31.5	31.5
15	31.8	31.8	31.8	31.8
20	32.9	32.9	32.9	32.9

25	33.8	33.8	33.8	33.8
30	34.9	34.9	34.9	34.9
35	35.1	35.1	35.1	35.1
40	35.3	35.3	35.3	35.3
45	35.6	35.6	35.6	35.6
50	35.9	35.9	35.9	35.9
55	36.3	36.3	36.3	36.3
60	36.7	36.7	36.7	36.7
65	36.9	36.9	36.9	36.9
70	37.4	37.4	37.4	37.4
75	37.6	37.6	37.6	37.6
80	38	38	38	38
85	38.8	38.8	38.8	38.8
90	39.7	39.7	39.7	39.7
95	39.8	39.8	39.8	39.8
100	40.4	40.4	40.4	40.4
105	40.9	40.9	40.9	40.9
110	41.5	41.5	41.5	41.5
115	42	42	42	42
120	42.9	42.9	42.9	42.9

Figure 3.13 shows the graph for median temperature analysis under no load – fan off condition for heat sink 1 and heat sink 2 respectively

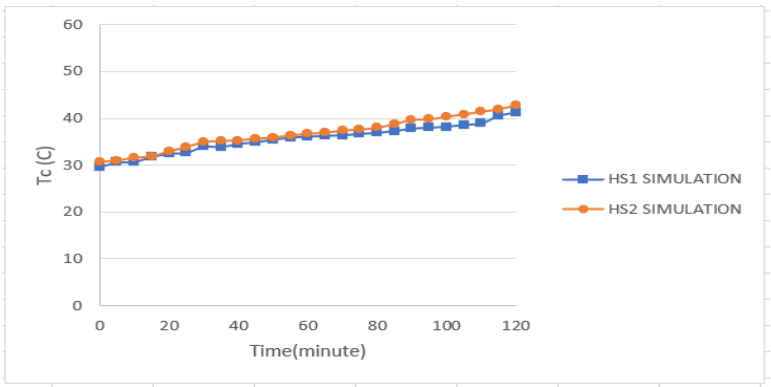

Fig. 3.13. Graph shows the median temperature measurements for HS1 and HS2 under no load and fan off condition

t = 60 minute

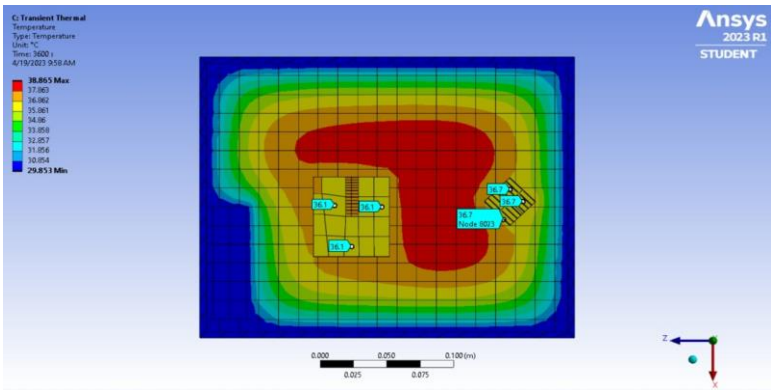

t = 120 minute

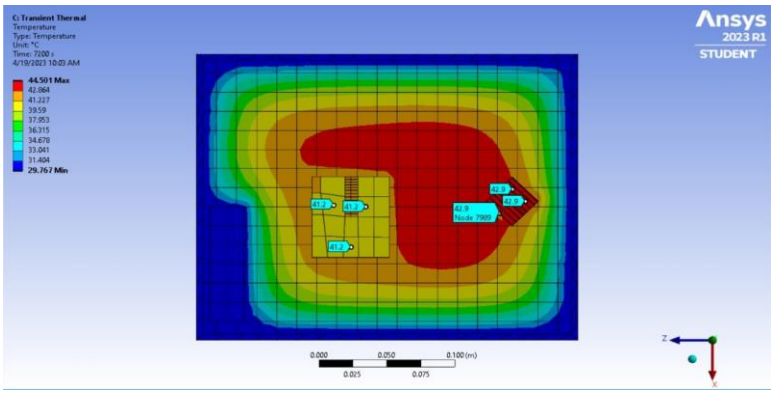

Fig. 3.14. Temperature contours obtained through simulation at different time periods

3(c): Under load condition; Fan off, with heat sink 1; Ambient temperature 29^0C

Table 3.11 show the results for heat sink 1 under load – fan off condition, the ambient temperature was 29^0C. Highest temperature at 120^{th} minute observed was 49.9^0C.

Table 3.11. Temperature measurements for HS1 under load and fan off condition

TIME (minute)	T1(Celsius)	T2(Celsius)	T3(Celsius)	Tc (Celsius)
0	30	30	30	30
5	30.7	30.7	30.7	30.7
10	31.5	31.5	31.5	31.5
15	31.9	31.9	31.9	31.9
20	32.8	32.8	32.8	32.8
25	33.6	33.6	33.6	33.6
30	34.2	34.2	34.2	34.2
35	34.8	34.8	34.8	34.8
40	35.4	35.4	35.4	35.4
45	36.6	36.6	36.6	36.6
50	37.5	37.5	37.5	37.5
55	38.5	38.5	38.5	38.5
60	39.9	39.9	39.9	39.9
65	40.4	40.4	40.4	40.4
70	41.3	41.3	41.3	41.3
75	42.7	42.7	42.7	42.7
80	43.9	43.9	43.9	43.9
85	45	45	45	45
90	46.2	46.2	46.2	46.2
95	46.9	46.9	46.9	46.9
100	47.5	47.5	47.5	47.5
105	47.9	47.9	47.9	47.9
110	48.4	48.4	48.4	48.4
115	48.7	48.7	48.7	48.7
120	49.9	49.9	49.9	49.9

3(d): Under load condition; Fan off, with heat sink 2; Ambient temperature 29^0C

Table 3.12 show the results for heat sink 2 under load – fan off condition, the ambient temperature was 29^0C. Highest temperature at 120^{th} minute observed was 52.5^0C.

Table 3.12. Temperature measurements for HS2 under load and fan off condition

TIME (minute)	T1(Celsius)	T2(Celsius)	T3(Celsius)	Tc (Celsius)
0	29.8	29.8	29.8	29.8
5	31.8	31.8	31.8	31.8
10	32.8	32.8	32.8	32.8
15	33.9	33.9	33.9	33.9
20	35.4	35.4	35.4	35.4
25	36.9	36.9	36.9	36.9
30	38.1	38.1	38.1	38.1
35	38.6	38.6	38.6	38.6
40	39.6	39.6	39.6	39.6
45	40.7	40.7	40.7	40.7
50	41.7	41.7	41.7	41.7
55	42.9	42.9	42.9	42.9
60	44.6	44.6	44.6	44.6
65	44.8	44.8	44.8	44.8
70	45.9	45.9	45.9	45.9
75	46.6	46.6	46.6	46.6
80	47.9	47.9	47.9	47.9
85	48.6	48.6	48.6	48.6
90	49.9	49.9	49.9	49.9
95	50.2	50.2	50.2	50.2
100	50.4	50.4	50.4	50.4
105	50.7	50.7	50.7	50.7
110	51.6	51.6	51.6	51.6
115	51.8	51.8	51.8	51.8
120	52.5	52.5	52.5	52.5

Figure 3.15 shows the graph for median temperature analysis under load – fan on condition for heat sink 1 and heat sink 2 respectively

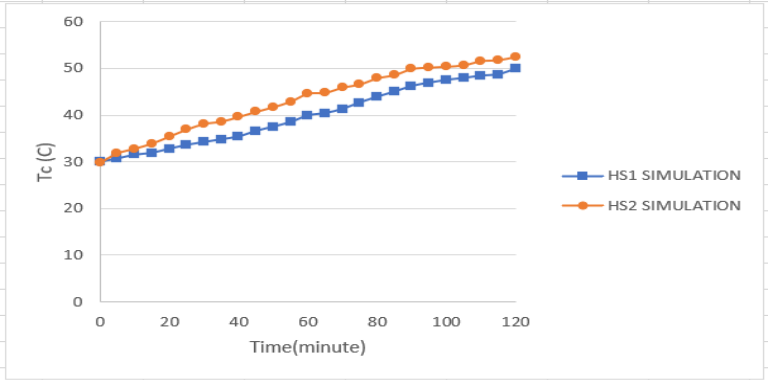

Fig. 3.15. Graph shows the median temperature measurements for HS1 and HS2 under load and fan off condition

t = 60 minute

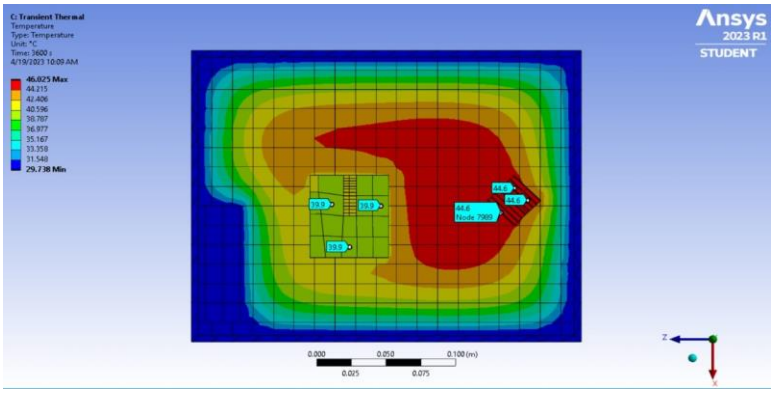

t = 120 minute

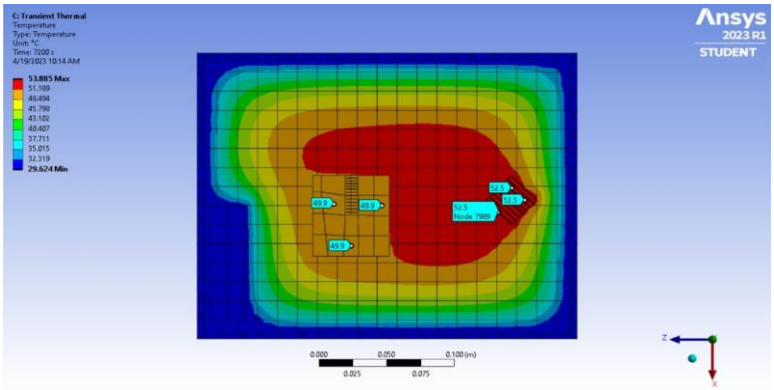

Fig. 3.16. Temperature contours obtained through simulation at different time periods

4(a): Under no load condition; Fan off, on microprocessor (heat sink 1 removed); Ambient temperature 29^0C

Table 3.13 show the results for microprocessor under no load – fan off condition, the ambient temperature was 29^0C. Highest temperature at 120^{th} minute observed was 46.6^0C.

Table 3.13. Temperature measurements for microprocessor under no load and fan off condition

TIME (minute)	T1(Celsius)	T2(Celsius)	T3(Celsius)	Tc (Celsius)
0	31	31	31	31
5	32.3	32.3	32.3	32.3
10	32.7	32.7	32.7	32.7
15	32.9	32.9	32.9	32.9
20	33.7	33.7	33.7	33.7
25	34.3	34.3	34.3	34.3
30	34.9	34.9	34.9	34.9
35	35.3	35.3	35.3	35.3
40	36.7	36.7	36.7	36.7
45	37.5	37.5	37.5	37.5
50	38.6	38.6	38.6	38.6
55	39.3	39.3	39.3	39.3
60	40	40	40	40
65	40.2	40.2	40.2	40.2
70	40.6	40.6	40.6	40.6
75	41.1	41.1	41.1	41.1
80	41.7	41.7	41.7	41.7
85	41.9	41.9	41.9	41.9
90	42.2	42.2	42.2	42.2
95	42.5	42.5	42.5	42.5
100	42.9	42.9	42.9	42.9
105	43.9	43.9	43.9	43.9
110	44.8	44.8	44.8	44.8
115	45.5	45.5	45.5	45.5

120	46.6	46.6	46.6	46.6

Figure 3.17 shows the graph for median temperature analysis under no load – fan off condition for microprocessor.

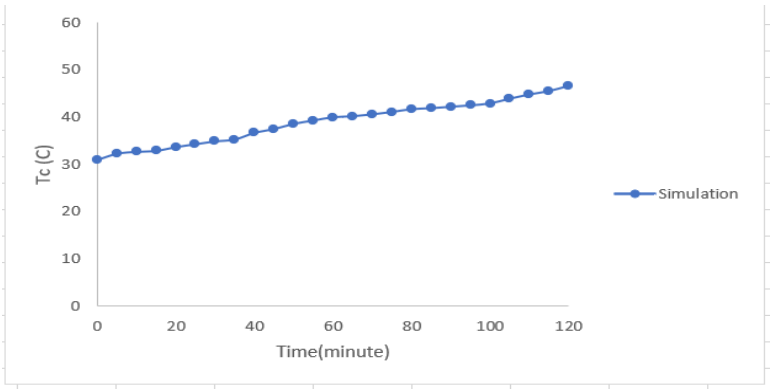

Fig. 3.17. Graph shows the median temperature measurements for microprocessor under no load and fan off condition

Figure 3.18 shows the thermal profile obtained through simulation under no load – fan off condition at different time period in the CPU chassis.

t = 60 minute

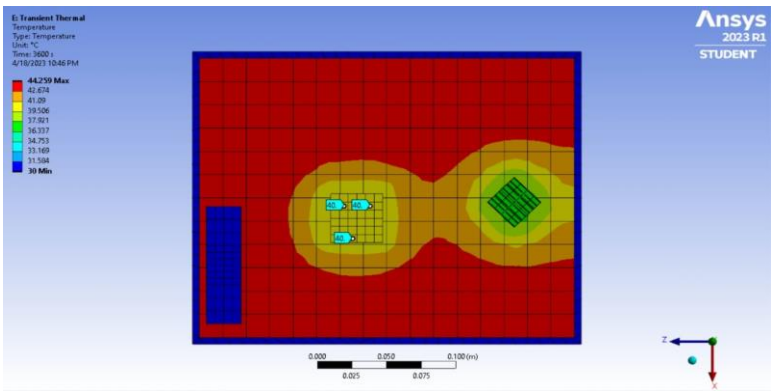

t = 120 minute

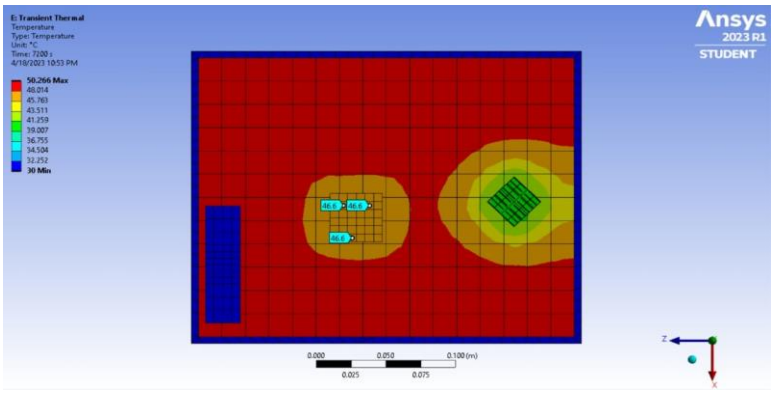

Fig. 3.18. Temperature contours obtained through simulation at different time periods

4(b): Under load condition; Fan off, on microprocessor (heat sink 1 removed); Ambient temperature 29^{0}C

Table 3.14 show the results for microprocessor under load – fan off condition, the ambient temperature was 30^{0}C. Highest temperature at 30th minute observed was 58^{0}C. It is to be noted that Intel Core i7 microprocessor can withstand up to a temperature range of 57^{0}C – 65^{0}C, so on reaching the temperature 58^{0}C at 30th minute simulation process was stopped.

Table 3.14. Temperature measurements for microprocessor under load and fan off condition

TIME (minute)	T1(Celsius)	T2(Celsius)	T3(Celsius)	Tc (Celsius)
0	31	31	31	31
5	39.3	39.3	39.3	39.3
10	44.4	44.4	44.4	44.4
15	47.5	47.5	47.5	47.5
20	50	50	50	50
25	54.5	54.5	54.5	54.5
30	58	58	58	58

Following figure 3.19 shows the median temperature analysis under load – fan off condition for microprocessor.

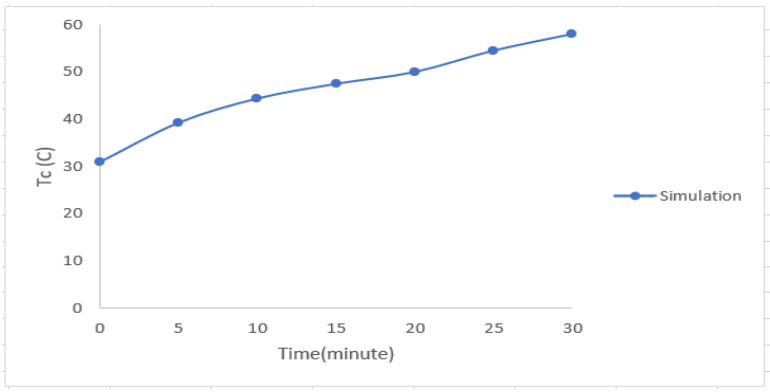

Fig. 3.19. Graph shows the median temperature measurements for microprocessor under load and fan off condition

Figure 3.20 shows the thermal profile obtained through simulation under load – fan off condition at different time period in the CPU chassis.

t = 10 minute

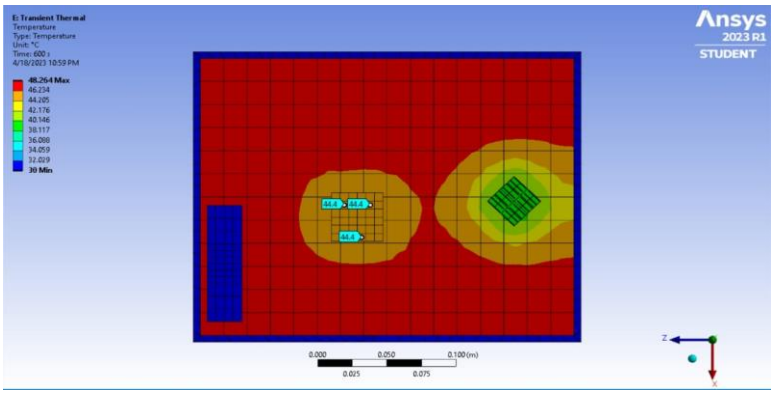

t = 30 minute

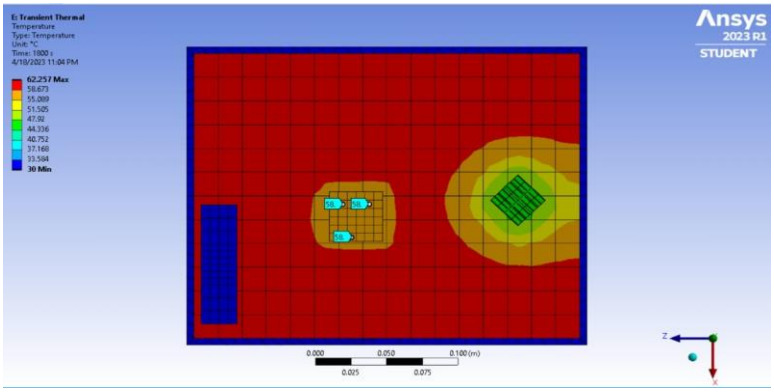

Fig. 3.20. Temperature contours obtained through simulation at different time periods

CHAPTER 4

EXPERIMENTAL METHOD

4.1. Methodology

The aim of this work is to find temperature at different points of heat sink and microprocessor of CPU under no load and load conditions with respect to time. Under load conditions three applications were running on the computer they are: Videos on YouTube, C++ infinite loop and MaxPayne game application. Experiment was conducted in four stages: 1) With heat sink and fan on; 2) With heat sink, fan on and in between placing an obstacle; 3) With heat sink and fan off; and finally, by 4) removing heat sink (on microprocessor) and fan off. Duration of the experiment was 2 hours for each condition. Ambient temperature was around 29^0C - 30^0C.

In this experiment Fluke Ti 450 thermal image camera is used to find temperatures at different locations and to capture thermal image. It offers a spectral range of 7.5µm to 14µm, image resolution of 320 × 240 pixels and an accuracy of $\pm 2^0$C. Using the method of three-point markers, temperature at three different locations can be calculated and the median temperature is calculated by default. T1, T2, T3 are the temperature taken at random locations and Tc is the median temperature.

The software used for this camera is SmartView software. It is installed on to the computer so that images taken can be downloaded from the camera.

For the experiment CPU model used was HP COMPAQ ELITE 8300 SFF and microprocessor installed is Intel(R) Core (TM) i7-3770 CPU @ 3.40GHz.

Figure 4.1 shows how the measurements are taken by the thermal camera

Fig. 4.1. Measurements taken with thermal camera

4.2. Experimental Results

5(a): Under no load condition; Fan on, with heat sink 1; Ambient temperature 29^0C

Table 4.1. show the results for heat sink 1 under no load – fan on condition, the ambient temperature was 29^0C. Highest temperature at 120^{th} minute observed was 29.5^0C.

Table 4.1. Temperature measurements for HS1 under no load and fan on condition

TIME (minute)	T1(Celsius)	T2(Celsius)	T3(Celsius)	Tc (Celsius)
0	29.9	29.9	30.1	29.9
5	29.4	29.3	29.8	29.5
10	29.6	29.5	29.3	29.5
15	30.1	29.9	29.8	29.7
20	29.8	29.7	29.9	29.5
25	30.1	29.9	29.8	29.9
30	29.5	29.4	29.8	29.4
35	29.7	29.8	29.6	29.7
40	29.8	29.9	29.7	29.6
45	29.5	29.8	30.1	29.2
50	29.7	29.6	29.9	29.3

55	29.8	29.9	29.6	29.4
60	29.4	29.4	29.8	29.3
65	29.8	29.7	29.7	29.8
70	29.9	29.8	29.7	29.3
75	29.8	29.9	29.8	29.6
80	29.7	29.8	29.8	29.3
85	29.8	29.9	29.7	29.5
90	29.3	29.7	30	29.3
95	29.8	29.9	29.8	29.2
100	29.7	29.9	29.8	29.6
105	29.8	29.9	29.6	29.7
110	29.9	29.6	29.5	29.3
115	29.5	29.8	29.6	29.2
120	29.5	29.7	30.1	29.5

Figure 4.2 shows the infrared thermal images for heat sink 1 under no load – fan on condition at different time periods.

t = 60 minutes

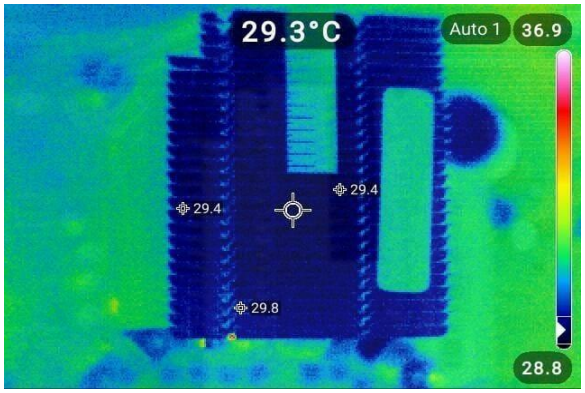

t = 120 minutes

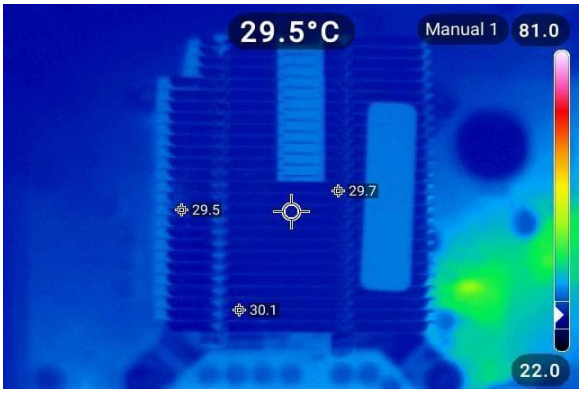

Fig. 4.2. Thermal images for HS1 under no load condition

5(b): Under no load condition; Fan on, with heat sink 2; Ambient temperature 29^0C

Table 4.2 show the results for heat sink 2 under no load – fan on condition, the ambient temperature was 29^0C. Highest temperature at 120^{th} minute observed was 31.8^0C.

Table 4.2 Temperature measurements for HS2 under no load and fan on condition

TIME (minute)	T1(Celsius)	T2(Celsius)	T3(Celsius)	Tc (Celsius)
0	29.9	29.9	30.1	29.9
5	29.4	29.3	29.8	29.5
10	29.6	29.5	29.3	29.5
15	30.1	29.9	29.8	29.7
20	29.8	29.7	29.9	29.5
25	30.1	29.9	29.8	29.9
30	29.5	29.4	29.8	29.4
35	29.7	29.8	29.6	29.7
40	29.8	29.9	29.7	29.6
45	29.5	29.8	30.1	29.2
50	29.7	29.6	29.9	29.3
55	29.8	29.9	29.6	29.4
60	29.4	29.4	29.8	29.3
65	29.8	29.7	29.7	29.8
70	29.9	29.8	29.7	29.3
75	29.8	29.9	29.8	29.6
80	29.7	29.8	29.8	29.3
85	29.8	29.9	29.7	29.5
90	29.3	29.7	30	29.3
95	29.8	29.9	29.8	29.2
100	29.7	29.9	29.8	29.6
105	29.8	29.9	29.6	29.7
110	29.9	29.6	29.5	29.3
115	29.5	29.8	29.6	29.2

120	29.5	29.7	30.1	29.5

Figure 4.3 shows the infrared thermal images for heat sink 2 under no load – fan on condition at different time periods.

t = 60 minutes

t = 120 minutes

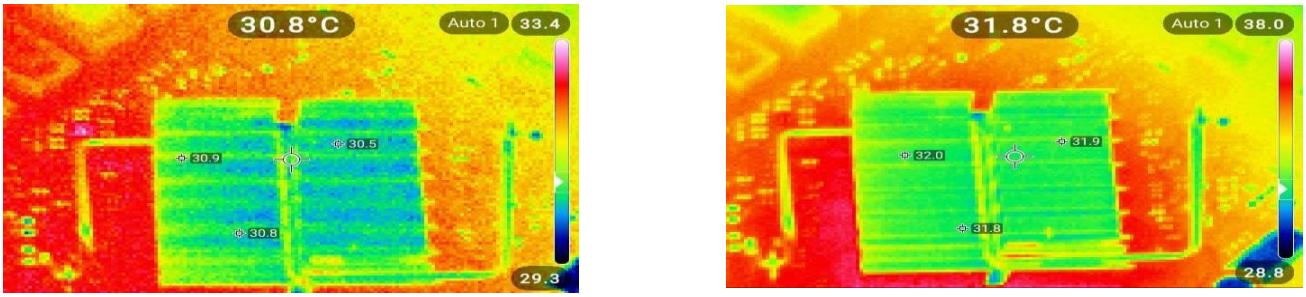

Fig. 4.3 Thermal images for HS2 under no load condition

Figure 4.4 shows the graph for median temperature measurements from experimental method for heat sink 1 and heat sink 2 under no load - fan on condition

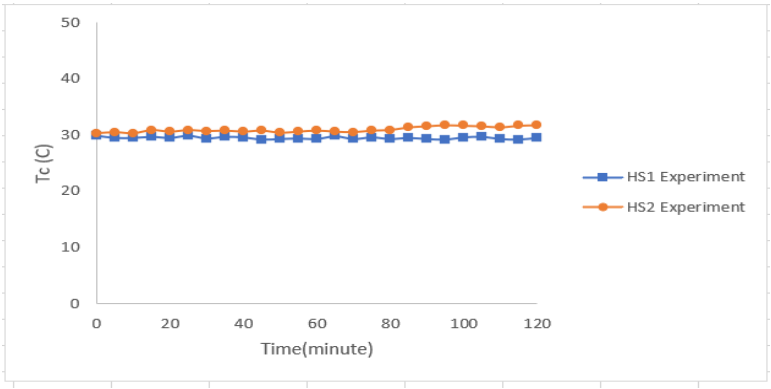

Fig. 4.4 Graph shows the median temperature measurements for HS1 and HS2 under no load and fan on condition

5(c): Under load condition; Fan on, with heat sink 1; Ambient temperature 29^{0}C

Table 4.3 show the results for heat sink 1 under load – fan on condition, the ambient temperature was 29^{0}C. Highest temperature at 120th minute observed was 45^{0}C.

Table 4.3. Temperature measurements for HS1 under load and fan on condition

Time(minute)	T1(Celsius)	T2(Celsius)	T3(Celsius)	Tc (Celsius)
0	30.9	30.3	30.4	30.3
5	31.4	31.1	31.2	31.2
10	31.7	31.5	31.6	31.5
15	32.3	32.2.	32.1	32.2
20	32.9	32.6	32.7	32.4
25	33.8	33.1	33.3	32.9
30	34.2	33.7	33.6	33.1
35	34.6	34.2	34.3	33.9
40	35.2	35.1	35.1	35.4
45	35.7	35.8	35.7	35.9
50	36.4	36.5	36.4	36.3
55	37.5	37.9	37.8	37.2
60	38.1	39.1	38.7	37.9
65	38.5	39.4	38.9	38.2
70	39.1	39.5	39.1	38.5
75	39.6	39.7	39.4	38.9
80	40.3	40.1	39.5	39.4
85	40.7	40.3	39.7	39.7
90	41	40.7	40.2	40
95	41.7	41.2	40.7	40.9
100	42.3	41.6	41.4	41.5
105	42.8	42.4	41.9	42.1
110	43.2	42.9	42.6	43.4
115	43.7	43.6	43.4	44.1
120	44.1	44.1	44.6	45

Figure 4.5 shows the infrared thermal images for heat sink 1 under load – fan on condition at different time periods.

t = 60 minutes

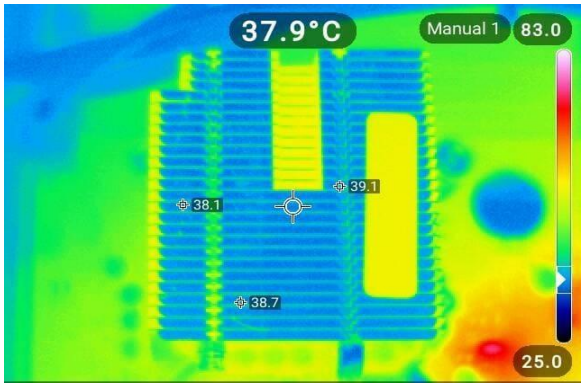

t = 120 minutes

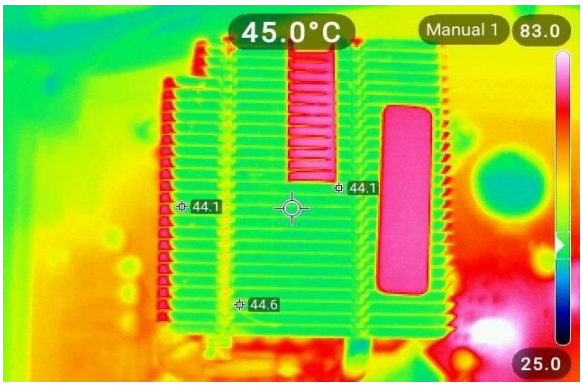

Fig. 4.5 Thermal images for HS1 under load condition

5(d): Under load condition; Fan on, with heat sink 2; Ambient temperature 29^{0}C

Table 4.4 show the results for heat sink 2 under load – fan on condition, the ambient temperature was 29^{0}C. Highest temperature at 120th minute observed was 47.5^{0}C.

Table 4.4. Temperature measurements for HS2 under load and fan on condition

Time(minute)	T1(Celsius)	T2(Celsius)	T3(Celsius)	Tc(Celsius)
0	29.5	29.3	29.6	29.3
5	30.2	30.6	30.5	30.4
10	30.9	31.4	31.2	31.3
15	31.7	32.1	32.8	32.1
20	32.8	33.2	33.5	33.2
25	34.1	34.3	34.3	34.1
30	35.3	35	35.5	35.2
35	36.1	35.9	36.4	36.1
40	37.2	36.8	37.1	37.3
45	38.3	37.6	37.9	38.1
50	39.1	38.7	38.9	39.4
55	39.7	39.1	39.5	40.5
60	40.5	39.5	40.1	41.9

65	41.8	40.7	40.9	42.3
70	42.5	41.9	41.7	42.7
75	43.1	42.4	42.2	42.9
80	43.6	43.5	43.8	43.7
85	43.9	44.3	44.6	44.2
90	44.3	45.1	45	44.5
95	45.2	45.7	45.6	45.1
100	46.1	46.3	46.1	45.9
105	46.8	46.9	46.8	46.5
110	47.4	47.3	47.4	46.9
115	47.8	47.9	47.7	47.1
120	48.1	48.3	48.1	47.5

Figure 4.6 shows the infrared thermal images for heat sink 2 under load – fan on condition at different time periods.

t = 60 minutes

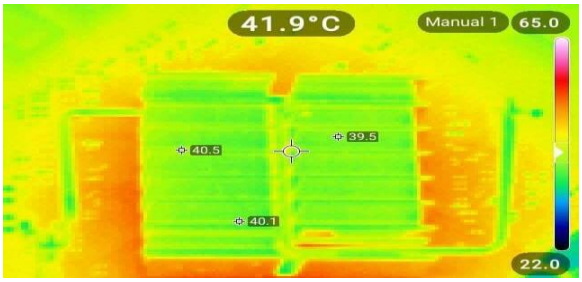

t = 120 minutes

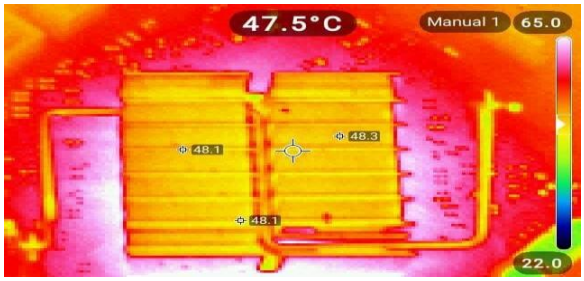

Fig. 4.6 Thermal images for HS2 under load condition

Following graph shows the median temperature measurements from experimental method for heat sink 1 and heat sink 2 under load - fan on condition.

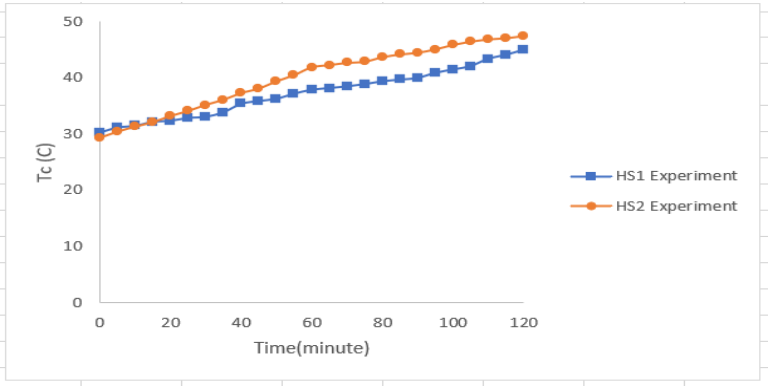

Fig. 4.7 Graph shows the median temperature measurements for HS1 and HS2 under load and fan on condition

2: With obstacle – Obstacle used for the experiment is book of dimension 105mm × 80mm × 2mm book was resting on its longest side of 105mm length. The obstacle was placed 24mm from the fan and was in between heat sink 1.

2(a): Under no load condition; With obstacle, Fan on, with heat sink 1; Ambient temperature 30^0C

Table 4.5 show the results for heat sink 1 under no load – fan on condition with obstacle, the ambient temperature was 29^0C. Highest temperature at 120^{th} minute observed was 34^0C.

Table 4.5 Temperature measurements for HS1 under no load, fan on and by placing an obstacle condition

Time(minute)	T1(Celsius)	T2(Celsius)	T3(Celsius)	Tc (Celsius)
0	31.8	30.9	30.9	31.1
5	31.7	30.8	31	31.3
10	31.4	31.3	31.7	31.2
15	31.2	31.5	31.7	31.3
20	31.9	31.8	32	32.3
25	32	32.2	32.4	32.2
30	32.3	32.6	32.8	32.1
35	32.3	32.4	32.5	32.1
40	32.2	32.5	32.3	32.1
45	32.4	32.1	32.6	32.8
50	32.5	32.3	32.5	32.4
55	32.3	32.6	32.4	32.9
60	32.5	33	32.6	32.4

65	32.8	32.9	32.7	32.8
70	33.1	33.2	33.4	33.1
75	33.5	33.3	33.6	33.8
80	33.8	33.7	33.8	33.9
85	33.7	33.8	33.6	33.8
90	33.9	34.2	34.2	33.7
95	34.1	34.3	34.4	34.2
100	34.2	34.4	34.1	34.3
105	34.3	34.5	34.3	34.2
110	34.1	34.2	34.4	34.4
115	34.1	34.1	34.2	34.3
120	34.3	34	34.1	34

t = 60 minutes

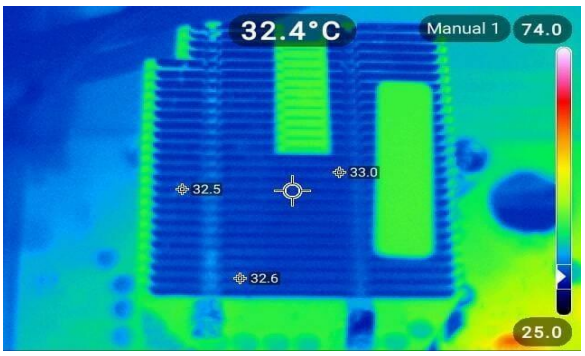

t = 120 minutes

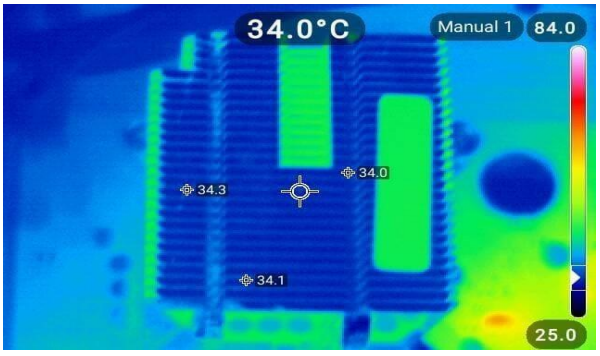

Fig 4.8. Thermal images for without running application with obstacle on HS1

2(b): Under no load condition; With obstacle, Fan on, with heat sink 2; Ambient temperature 30^0C

Table 4.6 show the results for heat sink 2 under no load – fan on condition with obstacle, the ambient temperature was 30^0C. Highest temperature at 120^{th} minute observed was 35.1^0C.

Table 4.6. Temperature measurements for HS2 under no load, fan on and by placing an obstacle condition

Time(minute)	T1(Celsius)	T2(Celsius)	T3(Celsius)	Tc (Celsius)
0	31.3	31.2	30.9	31.1
5	31.4	31.1	31	31.2
10	31.2	31.3	31.4	31.4
15	31.5	31.5	31.2	31.5
20	31.8	31.3	31.4	31.7
25	31.9	31.5	31.7	31.8
30	32	31.6	31.9	32
35	32.4	32.5	32	32.2
40	32.7	33.5	32.5	32.8
45	33.9	34.3	33.8	33.4
50	34.5	34.9	34.3	33.9
55	34.8	35.2	34.9	34.7
60	35.2	35.9	35.6	34.8
65	35.4	35.2	35.3	34.2
70	35.6	35.4	35.2	34.6
75	35.2	35.3	35.6	34.8
80	35.1	35.6	34.9	34.9
85	35.4	35.1	34.5	35.3
90	35.2	35.9	34.7	35.4
95	35.6	35.2	34.3	35.2
100	35.4	35.4	34.1	35.6
105	35.2	35.1	34.8	35.4
110	35.4	35.5	34.5	35.7
115	35.1	35.1	34.2	35.2
120	35.3	35	34	35.1

t = 60 minutes t = 120 minutes

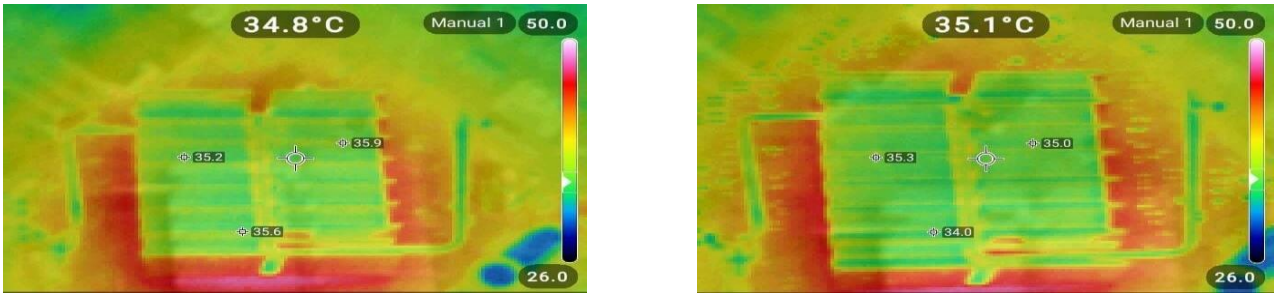

Fig. 4.9. Thermal images for without running application with obstacle on HS2

Figure 4.10 shows the graph for median temperature measurements from experimental method for heat sink 1 and heat sink 2 under no load - fan on condition with obstacle.

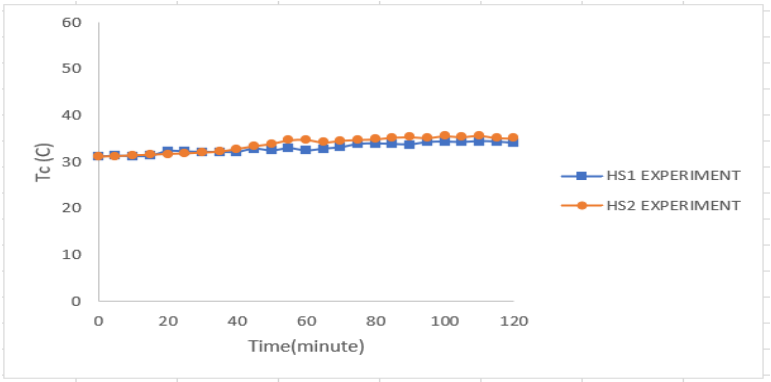

Fig. 4.10. Graph shows the median temperature measurements for HS1 and HS2 under no load and fan on condition with obstacle

2(c): Under load condition; With obstacle, Fan on, with heat sink 1; Ambient temperature 30^0C

Table 4.7 shows the results for heat sink 1 under no load – fan on condition with obstacle, the ambient temperature was 30^0C. Highest temperature at 120^{th} minute observed was 47.7^0C.

Table 4.7. Temperature measurements for HS1 under load, fan on and by placing an obstacle condition

Time(minute)	T1(Celsius)	T2(Celsius)	T3(Celsius)	Tc (Celsius)
0	29.7	29.8	29.4	29.5
5	30.1	30.2	30.7	30.5
10	31.4	31.3	31.5	31.8
15	32.8	32.3	32.4	32.4
20	33.1	33.2	33.5	33.6
25	33.7	33.9	34	33.9

30	34	34.1	34.8	34.4
35	34.6	34.3	34.9	34.5
40	34.8	34.5	34.9	34.7
45	35.6	35.1	35.5	35.9
50	36.2	36	36.4	36.3
55	36.7	36.3	36.8	36.1
60	37	37.4	37.4	37
65	38	38.1	38.4	38.2
70	39.1	39.2	39.3	39.4
75	40.6	40.5	40.8	40.4
80	41.3	41.2	41.7	41.5
85	42.8	42.3	42.5	42.3
90	43.3	43	43.8	43.1
95	44.2	44.3	44.7	44.5
100	44.7	44.6	44.8	44.9
105	45.4	45.1	45.4	45.3
110	46.8	46.2	46.3	46.9
115	47.5	47.2	47.6	47.2
120	48.4	48.1	48.7	47.7

t = 60 minutes

t = 120 minutes

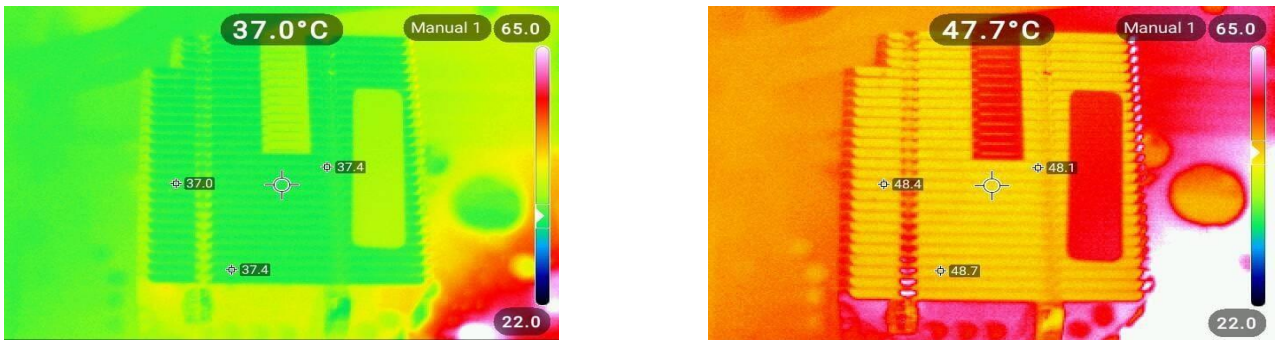

Fig. 4.11. Thermal images for running application with obstacle on HS1

2(d): Under load condition; With obstacle, Fan on, with heat sink 2; Ambient temperature 30^0C

Table 4.8 show the results for heat sink 2 under load – fan on condition with obstacle, the ambient temperature was 30^0C. Highest temperature at 120^{th} minute observed was 49.6^0C.

Table 4.8. Temperature measurements for HS2 under load, fan on and by placing an obstacle condition

Time(minute)	T1(Celsius)	T2(Celsius)	T3(Celsius)	Tc (Celsius)
0	30.1	30.2	30.1	30
5	30.3	30.5	30.2	30.7
10	31.2	31.4	31.7	31.4
15	32.2	32.6	32.5	32.6
20	33.7	33.1	33.4	33.8
25	34.9	34.6	34.8	34.1
30	36.1	36.4	35.2	35.5
35	36.3	36.5	35.4	35.8
40	36.7	36.6	36.2	36.4
45	37.3	37.1	37.4	37.7
50	38.2	38.3	38.2	38.1
55	39.4	39.3	39.1	39.3
60	39.4	39.8	39	39.9
65	40.1	40.4	40.2	40.3
70	41.3	41.2	41.4	41.2
75	42.6	42.4	42.5	42.4
80	43.3	43.1	43.5	43.1
85	43.7	43.9	43.9	43.6
90	44.3	45.1	45	44.5
95	45.2	45.5	45.4	45.3
100	46.1	46.4	46.3	46.7
105	47.6	47.8	47.9	47.2
110	48.9	48.7	48.6	48.1
115	49.9	49.7	49.8	48.9
120	50.5	50.6	50.9	49.6

t = 60 minutes

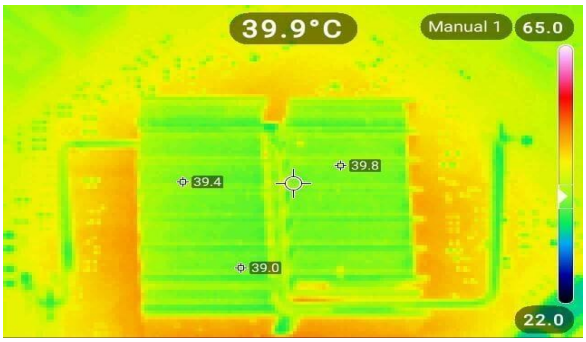

t = 120 minutes

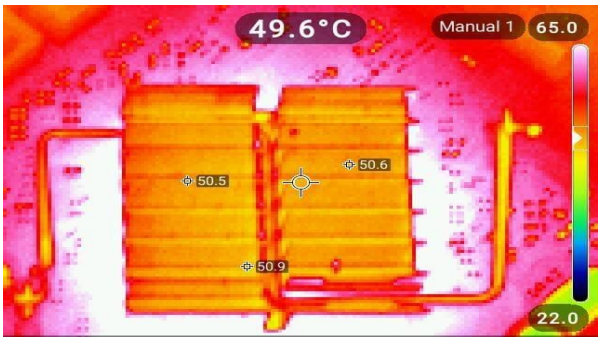

Fig. 4.12. Thermal images for running application with obstacle on HS2

Figure 4.13 shows the graph for median temperature measurements from experimental method for heat sink 1 and heat sink 2 under load - fan on condition with obstacle.

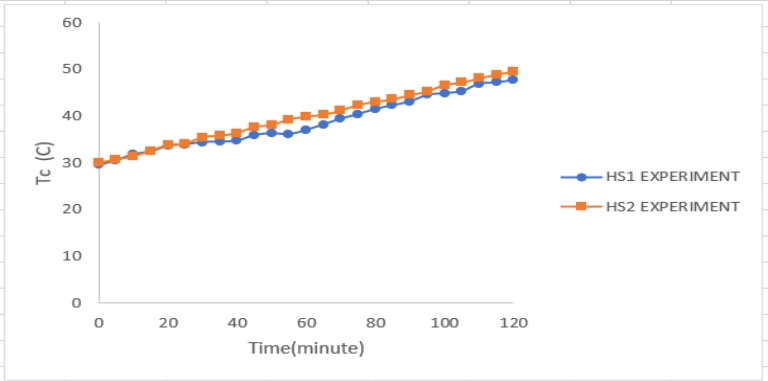

Fig. 4.13. Graph shows the median temperature measurements for HS1 and HS2 under load and fan on condition with obstacle

3(a): Under no load condition; Fan off, with heat sink 1; Ambient temperature 29^{0}C

Table 4.9 show the results for heat sink 1 under no load – fan off condition with, the ambient temperature was 29^{0}C. Highest temperature at 120th minute observed was 40^{0}C.

Table 4.9. Temperature measurements for HS1 under no load and fan off condition

Time(minute)	T1(Celsius)	T2(Celsius)	T3(Celsius)	Tc(Celsius)
0	29.7	29.5	29.9	29.5
5	30.2	30.6	30.2	30.4
10	30.8	30.6	30.4	30.7
15	31.3	31.1	31.7	31.8
20	31.7	31.8	31.9	32.5

25	32.4	32	32.7	33.4
30	32.8	32.1	33.7	34
35	33.5	33.4	33.9	34.4
40	34.3	34.2	34.3	34.6
45	34.7	34.8	34.6	34.9
50	35.1	35.4	35.5	35.2
55	35.5	35.7	35.9	35.5
60	35.8	36	36.1	35.8
65	36.1	36.2	36.3	36.1
70	36.3	36.4	36.4	36.3
75	36.5	36.5	36.7	36.4
80	36.8	36.7	36.9	36.6
85	37	37	37.3	37.1
90	37.2	37.1	37.8	37.2
95	37.4	37.5	37.9	37.5
100	37.6	37.7	38	37.9
105	38.3	38.5	38.4	38.6
110	39.3	38.9	39.5	39.4
115	40.5	39.1	40.5	39.8
120	41.2	39.3	40.7	40

t = 60 minutes

t = 120 minutes

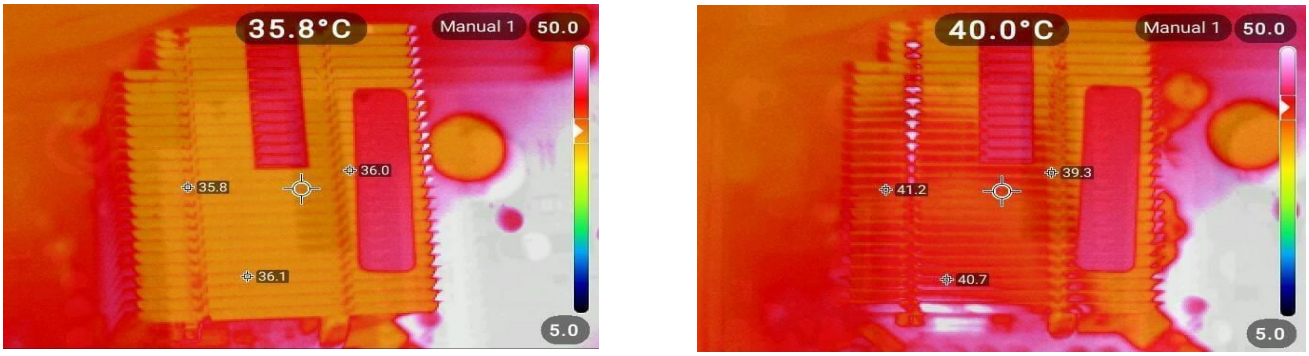

Fig. 4.14. Thermal images for fan off without running application on HS1

3(b): Under no load condition; Fan off, with heat sink 2; Ambient temperature 29^0C

Table 4.10 show the results for heat sink 2 under no load – fan off condition with, the ambient temperature was 29^0C. Highest temperature at 120^{th} minute observed was 42.9^0C.

Table 4.10. Temperature measurements for HS2 under no load and fan off condition

Time(minute)	T1(Celsius)	T2(Celsius)	T3(Celsius)	Tc(Celsius)
0	30.6	30.5	30.5	30.4
5	30.9	30.8	30.7	30.7
10	31.3	31.5	31.5	31.4
15	31.5	31.6	31.7	31.8
20	32.6	32.7	32.8	32.9
25	33.8	33.8	33.7	33.6
30	34.9	34.5	34.2	34
35	35	34.9	34.8	34.8
40	35.1	35.2	35.3	35.2
45	35.3	35.4	35.5	35.6
50	35.8	35.9	35.7	35.8
55	36.2	36.3	36.2	36.1
60	36.7	36.5	36.4	36.4
65	36.9	36.8	36.8	36.9
70	37.2	37.3	37.4	37.3
75	37.4	37.4	37.5	37.6
80	37.8	37.9	37.9	38
85	38.5	38.8	38.4	38.4
90	39	39.7	38.6	38.8
95	39.8	39.8	39.5	39.6
100	40.4	40.3	40.3	40.4
105	40.7	40.8	40.9	40.8
110	41.5	41.4	41.5	41.5
115	42	41.9	41.7	42
120	42.4	42.8	41.9	42.9

t = 60 minutes

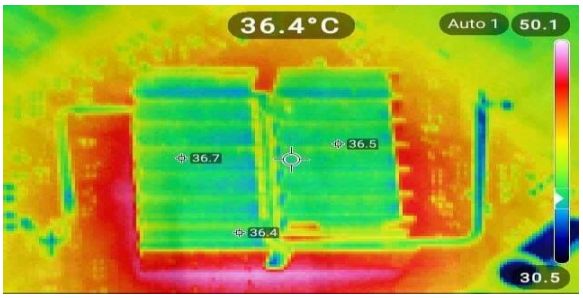

t = 120 minutes

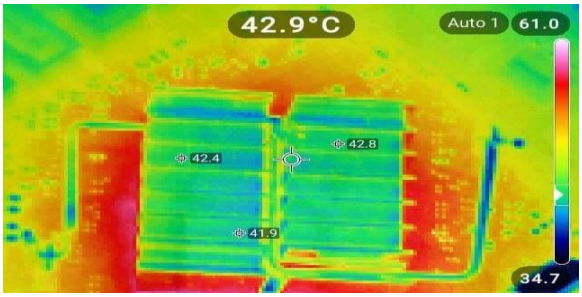

Fig. 4.15. Thermal images for fan off without running application on HS2

Figure 4.16 shows the median temperature measurements from experimental method for heat sink 1 and heat sink 2 under no load - fan off condition

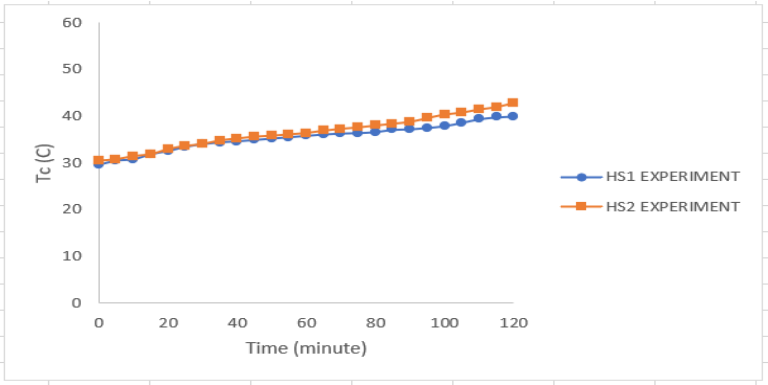

Fig. 4.16. Graph shows the median temperature measurements for HS1 and HS2 under no load and fan off condition

3(c): Under load condition; Fan off, with heat sink 1; Ambient temperature 29^{0}C

Table 4.11 show the results for heat sink 1 under no load – fan off condition with, the ambient temperature was 29^{0}C. Highest temperature at 120th minute observed was 48.2^{0}C.

Table 4.11. Temperature measurements for HS1 under load and fan off condition

Time(minute)	T1(Celsius)	T2(Celsius)	T3(Celsius)	Tc (Celsius)
0	29.8	30.3	30	29.8
5	30.4	30.5	30.7	30.7
10	31.1	31.2	31.5	31.4
15	31.8	31.6	31.9	31.7
20	32.3	32.8	32.8	32.4
25	32.8	33.6	33.6	32.8

30	33.5	34.2	34.1	33
35	34.2	34.8	34.8	34.3
40	35	35.4	35.4	35.1
45	36.2	36.6	36.5	36.3
50	37.4	37.5	37.4	37.2
55	38.5	38.1	37.8	37.9
60	39.9	38.8	38.4	38.4
65	40.4	39.9	39.9	39.8
70	41.3	41.1	41	41.2
75	42.7	42.5	42.4	42
80	43.9	43.8	43.6	43.6
85	45	44.9	44.7	44.7
90	46.2	46	45.9	45.2
95	46.5	46.9	46.5	45.5
100	46.9	47.5	47.3	46
105	47.3	47.9	47.9	46.6
110	47.5	48.2	48.4	47.1
115	47.8	48.7	48.6	47.5
120	48	49.9	49.7	48.2

t = 60 minutes

t = 120 minutes

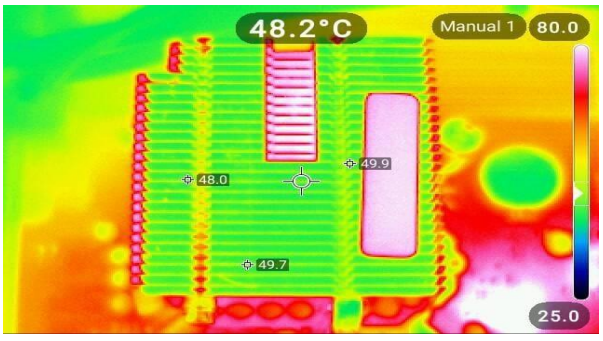

Fig. 4.17. Thermal images for fan off with running application on HS1

3(d): Under load condition; Fan off, with heat sink 2; Ambient temperature 29^0C

Table 4.12 show the results for heat sink 2 under load – fan off condition with, the ambient temperature was 29^0C. Highest temperature at 120^{th} minute observed was 52.3^0C.

Table 4.12 Temperature measurements for HS2 under load and fan off condition

Time(minute)	T1(Celsius)	T2(Celsius)	T3(Celsius)	Tc (Celsius)
0	29.7	29.5	29.8	29.7
5	31.5	31.8	31.7	31.7
10	32.4	32.6	32.6	32.8
15	33.9	33.8	33.7	33.9
20	35.1	35.1	35.3	35.4
25	36.8	36.9	36.4	36.5
30	37.7	38.1	36.9	37.1
35	38.6	38.6	37.8	38.5
40	39.4	39.6	39.1	39.4
45	40.6	40.4	40.7	40.7
50	41.4	41.6	41.4	41.7
55	42.7	42.8	42.6	42.9
60	43.5	43.5	43.5	44.6
65	44.6	44.4	44.8	44.7
70	45.8	45.7	45.9	45.8
75	46.4	46.6	46.3	46.6
80	47.5	47.9	47.9	47.6
85	47.9	48.5	48.6	48.1
90	48.2	49.9	49.2	48.6
95	48.7	50.2	49.5	49.1
100	49.6	50.4	49.9	49.8
105	50.5	50.6	50.5	50.7
110	51.4	51.4	51.6	51.4
115	51.7	51.8	51.8	51.6
120	52.5	52.2	52.4	52.3

t = 60 minutes t = 120 minutes

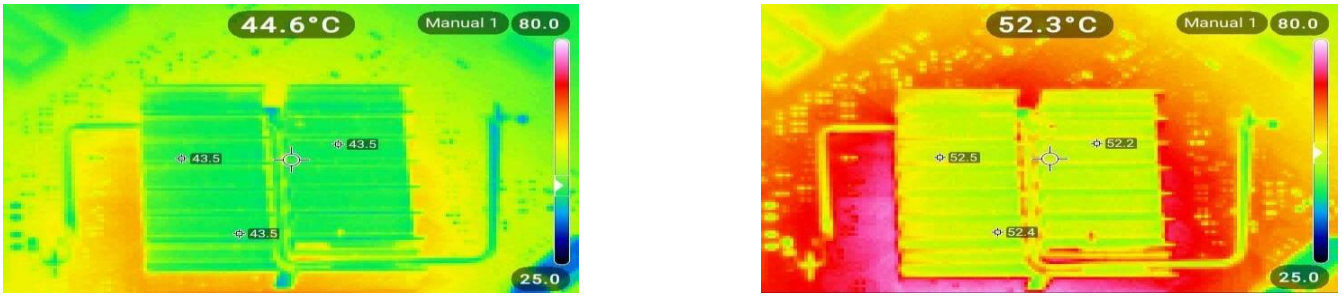

Fig. 4.18. Thermal images for fan off with running application on HS2

Figure 4.19 graph shows the median temperature measurements from experimental method for heat sink 1 and heat sink 2 under load - fan off condition

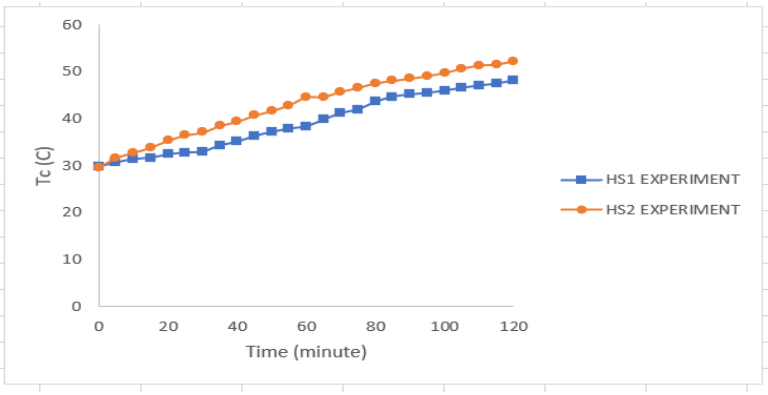

Fig. 4.19. Graph shows the median temperature measurements for HS1 and HS2 under no load and fan off condition

4(a): Under no load condition; Fan off, on microprocessor (heat sink 1 removed); Ambient temperature 30^{0}C

Table 4.13 show the results for microprocessor under no load – fan off condition, the ambient temperature was 30^{0}C. Highest temperature at 120th minute observed was 45.6^{0}C.

Table 4.13. Temperature measurements for microprocessor under no load and fan off condition

Time(minute)	T1(Celsius)	T2(Celsius)	T3(Celsius)	Tc (Celsius)
0	31.1	31	31.2	31
5	32.3	31.6	32.1	31.7
10	32.7	32.3	32.7	32.4
15	33.4	32.9	33.4	33.1

20	33.7	33.4	33.7	33.6
25	34.3	33.9	33.9	33.8
30	34.9	34.6	34	34.1
35	35.2	35.3	34.7	34.4
40	35.8	36.7	35.3	35.2
45	36.4	37.5	36.4	36.1
50	36.9	38.6	37.6	37.2
55	37.2	39.3	38.3	38.4
60	37.9	40	39.7	39.2
65	38.6	40.2	40.2	39.5
70	39.4	40.3	40.6	39.9
75	40.1	40.6	41.1	40.2
80	40.4	40.8	41.7	40.8
85	40.9	41	41.9	41.2
90	41.4	41.2	42.2	41.6
95	41.9	42.3	42.5	42.2
100	42.7	42.8	42.9	43.4
105	43.5	43.4	43.2	43.9
110	44.8	44.1	43.9	44.2
115	45.5	44.7	44.6	44.8
120	46.6	45.4	45.7	45.6

Figure 4.20 shows graph for the median temperature analysis under no load – fan off condition for microprocessor.

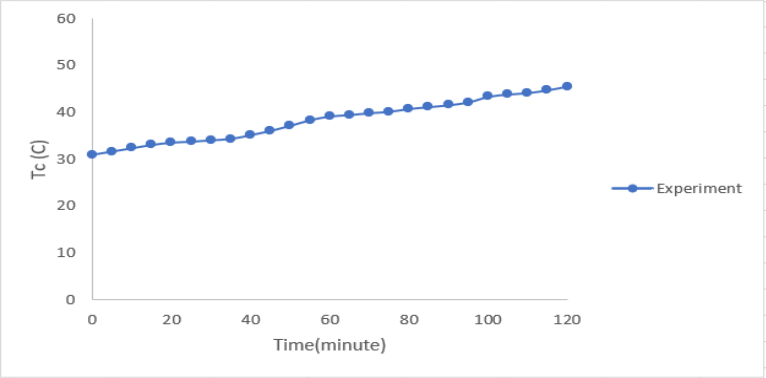

Fig. 4.20. Graph shows the median temperature measurements for microprocessor under no load and fan on condition

Figure 4.21. shows the infrared thermal images for microprocessor under no load – fan off condition at different time periods.

t = 60 minutes t = 120 minutes

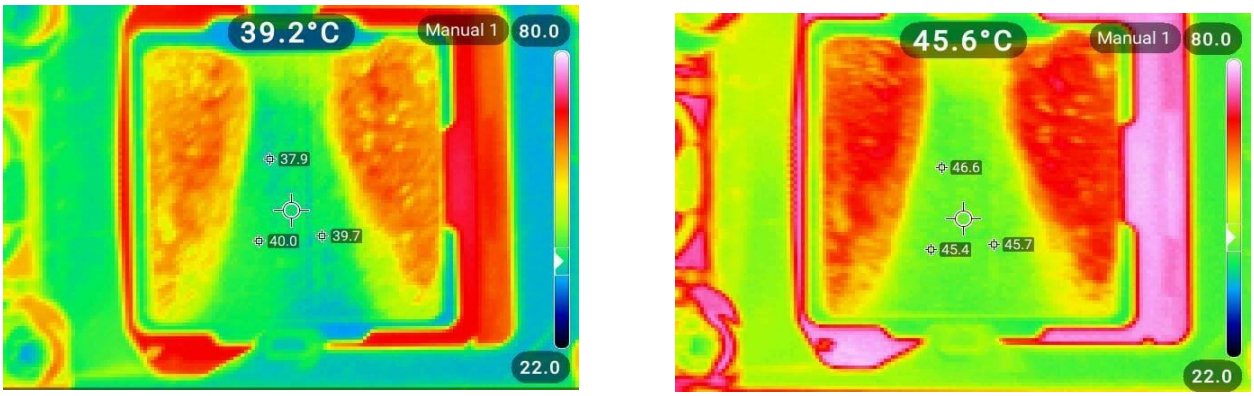

Fig. 4.21. Thermal images for microprocessor under no load condition

4(b): Under load condition; Fan off, on microprocessor (heat sink 1 removed); Ambient temperature 30^{0}C

Table 4.14 show the results for microprocessor under load – fan off condition, the ambient temperature was 30^{0}C. Highest temperature at 30th minute observed was 57.2^{0}C. It was observed that temperature rises up rapidly to 57.2^{0}C within short period of time, causing computer to shut down automatically in order to cool down and prevent damage to the computer.

Table 4.14. Temperature measurements for microprocessor under load and fan off condition

Time(minute)	T1(Celsius)	T2(Celsius)	T3(Celsius)	Tc (Celsius)
0	31.6	31.4	31.2	31

5	39.3	38.8	37.6	37.8
10	44.4	42.5	42.6	43
15	47.5	47.2	47.8	47.9
20	50.4	50.9	50	51.5
25	53.3	54.5	53.2	53.7
30	58.9	59.3	61	57.2

Figure 4.22 shows the graph for median temperature analysis under load – fan on condition for microprocessor.

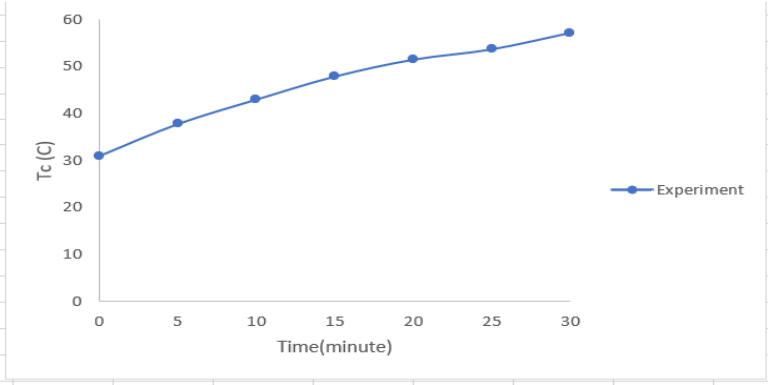

Fig. 4.22. Graph shows the median temperature measurements for microprocessor under no load and fan off condition

Figure 4.23. shows the infrared thermal images for microprocessor under load – fan on condition at different time periods

t = 10 minutes

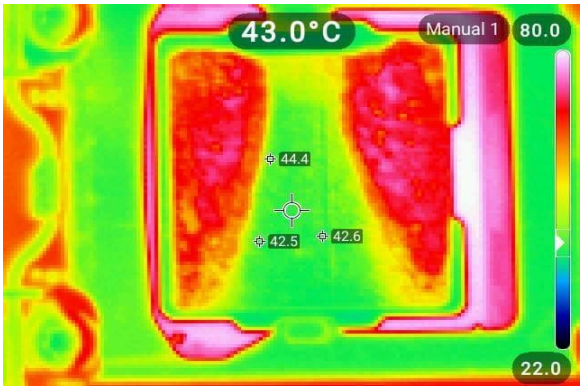

t = 30 minutes

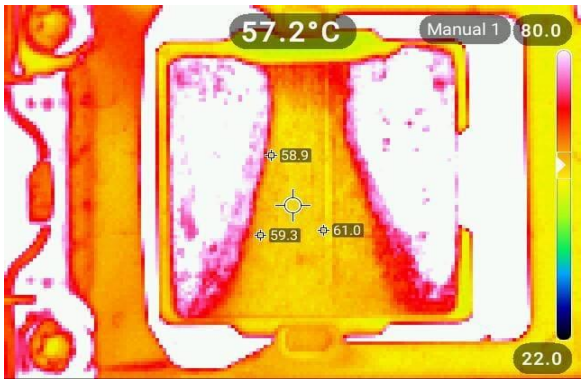

Fig. 4.23. Thermal images for microprocessor fan off with running application

CHAPTER 5

SIMULATION AND EXPERIMENTAL ANALYSIS

- Under no load condition; Fan on, with heat sink 1; Ambient temperature 29^0C: From the analysis for heat sink 1 under no load condition with fan on, the deviations between the simulation and experimental analysis are ranging from 0% to 3.08%. (Fig. 5.1)
- Under no load condition; Fan on, with heat sink 2; Ambient temperature 29^0C: From the analysis for heat sink 2 under no load condition with fan on, the deviations between the simulation and experimental analysis are ranging from 0% to 0.99%. (Fig. 5.1)
- Under load condition; Fan on, with heat sink 1; Ambient temperature 29^0C: From the analysis for heat sink 1 under load condition with fan on, the deviations between the simulation and experimental analysis are ranging from 0% to 3.32%. (Fig. 5.2)
- Under load condition; Fan on, with heat sink 2; Ambient temperature 30^0C: From the analysis for heat sink 2 under load condition with fan on, the deviations between the simulation and experimental analysis are ranging from 0% to 3.32%. (Fig. 5.2)
- Under no load condition; Fan on, with heat sink 1 and in between an obstacle; Ambient temperature 30^0C: From the analysis for heat sink 1 under no load condition with fan on, the deviations between the simulation and experimental analysis are ranging from 0% to 2.18% (Fig. 5.3)
- Under no load condition; Fan on, with heat sink 2 and in between an obstacle; Ambient temperature 30^0C: From the analysis for heat sink 2 under no load condition with fan on, the deviations between the simulation and experimental analysis are ranging from 0% to 3.5%. (Fig. 5.3)
- Under load condition; Fan on, with heat sink 1 and in between an obstacle; Ambient temperature 30^0C: From the analysis for heat sink 1 under load condition with fan on, the deviations between the simulation and experimental analysis are ranging from 0% to 1.94% (Fig. 5.4)
- Under load condition; Fan on, with heat sink 2 and in between an obstacle; Ambient temperature 30^0C: From the analysis for heat sink 2 under load condition with fan on, the

deviations between the simulation and experimental analysis are ranging from 0% to 2.54% (Fig. 5.4)

- Under no load condition; Fan off, with heat sink 1; Ambient temperature 29^0C: From the analysis for heat sink 1 under no load condition with fan off, the deviations between the simulation and experimental analysis are ranging from 0% to 2.1% (Fig. 5.5)
- Under no load condition; Fan off, with heat sink 2; Ambient temperature 29^0C: From the analysis for heat sink 1 under load condition with fan off, the deviations between the simulation and experimental analysis are ranging from 0% to 2.65% (Fig. 5.5)
- Under load condition; Fan off, with heat sink 1; Ambient temperature 29^0C: From the analysis for heat sink 1 under load condition with fan off, the deviations between the simulation and experimental analysis are ranging from 0% to 2.44% (Fig. 5.6)
- Under load condition; Fan off, with heat sink 2; Ambient temperature 29^0C: From the analysis for heat sink 2 under load condition with fan off, the deviations between the simulation and experimental analysis are ranging from 0% to 2.7% (Fig. 5.6)
- Under no load condition; Fan off, on microprocessor (heat sink 1 removed); Ambient temperature 30^0C: From the analysis for microprocessor under no load condition by disconnecting the fan, the deviations between the simulation and experimental analysis are ranging from 0% to 4.26%. (Fig. 5.7)
- Under load condition; Fan off, on microprocessor (heat sink 1 removed); Ambient temperature 30^0C: From the analysis for microprocessor under load condition by disconnecting the fan, the deviations between the simulation and experimental analysis are ranging from 0% to 3.97%. (Fig. 5.8)

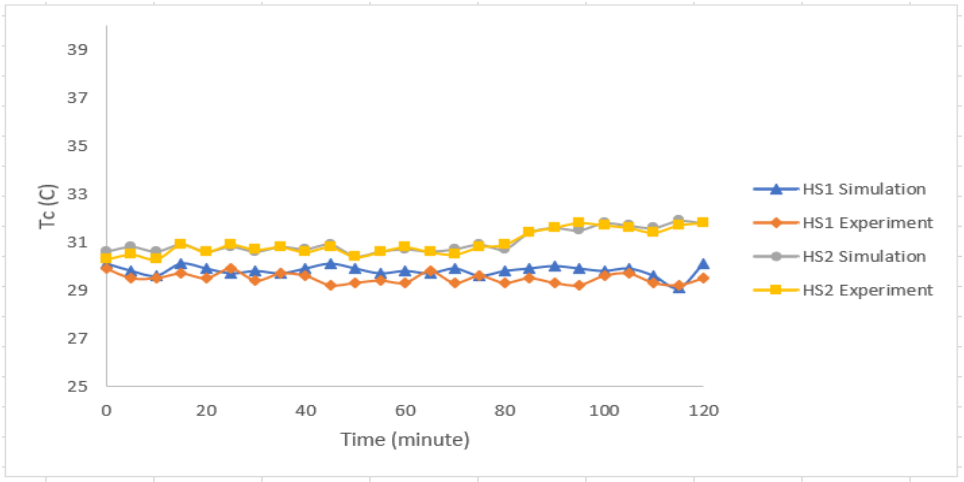

Fig. 5.1. Graph for the temperature analysis of heat sink 1 and heat sink 2 under no load and fan on condition

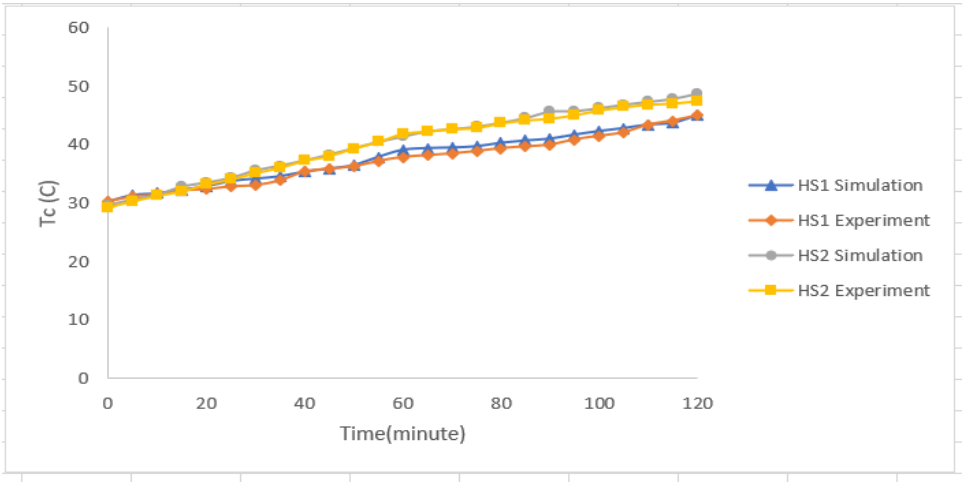

Fig. 5.2. Graph for the temperature analysis of heat sink 1 and heat sink 2 under load and fan on condition

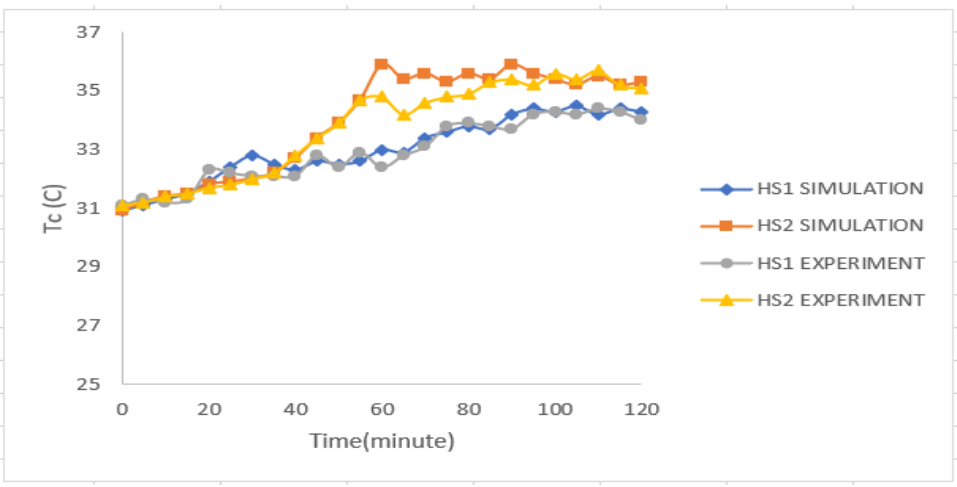

Fig. 5.3. Graph for the temperature analysis of heat sink 1 and heat sink 2 under no load, fan on and in between an obstacle.

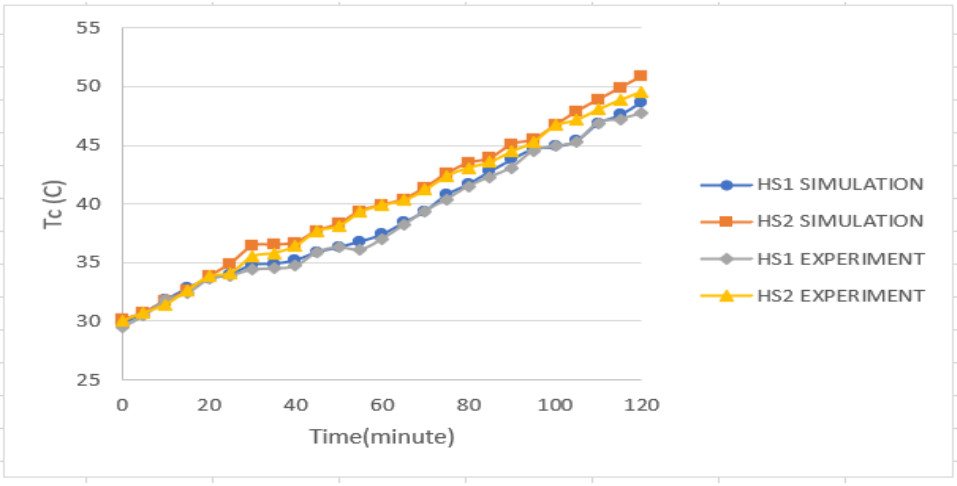

Fig. 5.4. Graph for the temperature analysis of heat sink 1 and heat sink 2 under load, fan on and in between an obstacle.

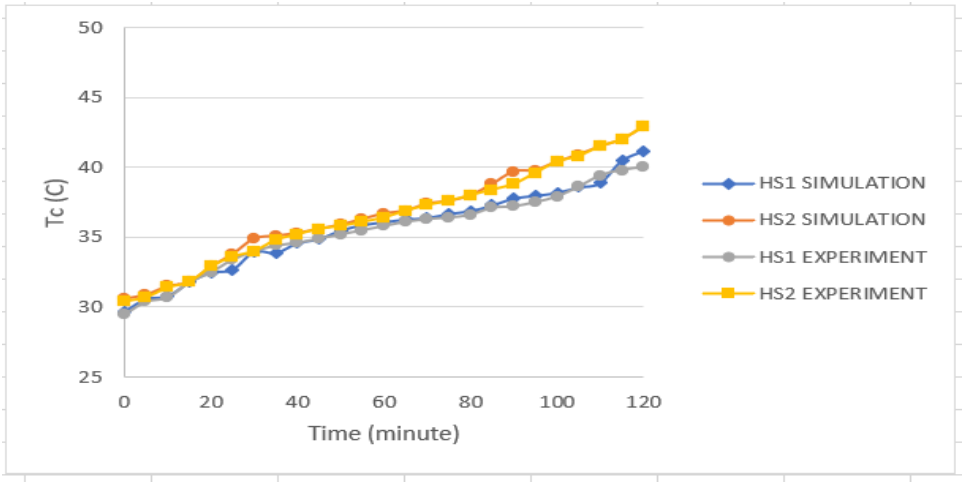

Fig. 5.5. Graph for the temperature analysis of heat sink 1 and heat sink 2 under no load and fan off condition.

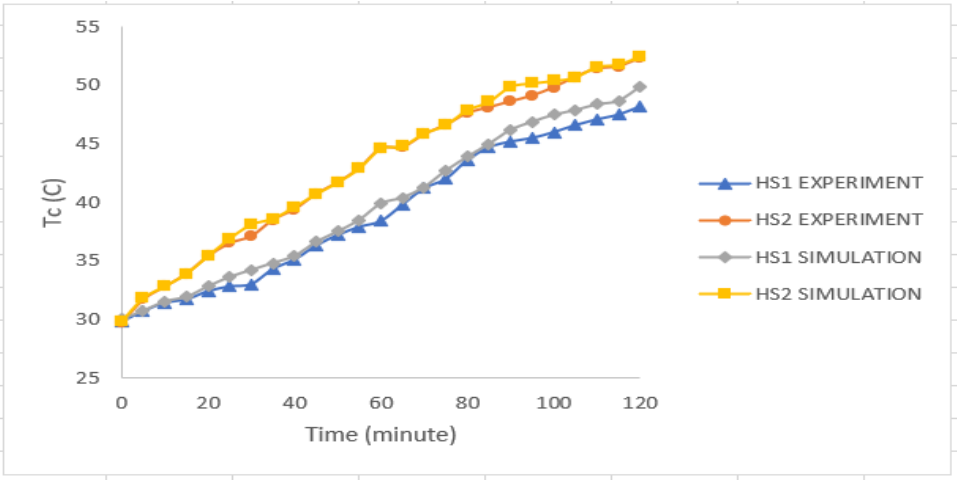

Fig. 5.6. Graph for the temperature analysis of heat sink 1 and heat sink 2 under load and fan off condition.

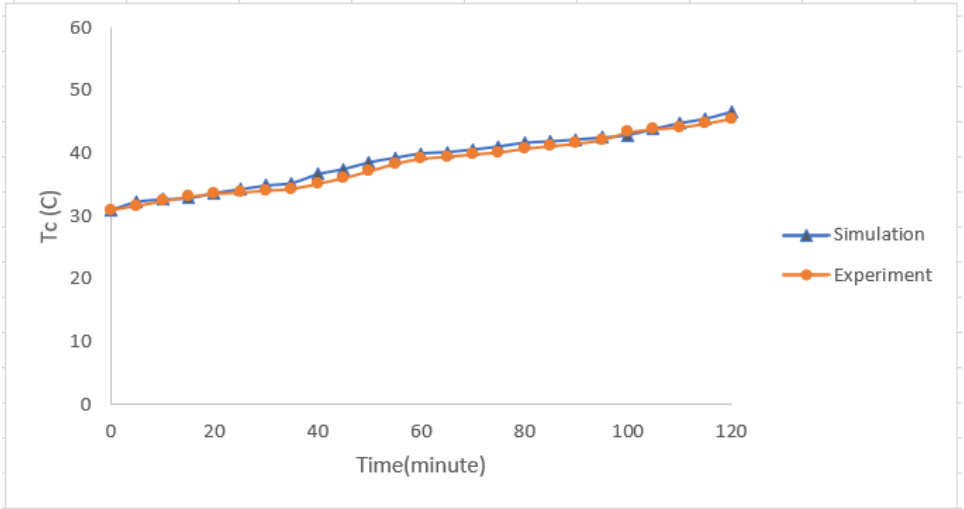

Fig. 5.7. Graph for the temperature analysis of microprocessor under no load and fan off condition

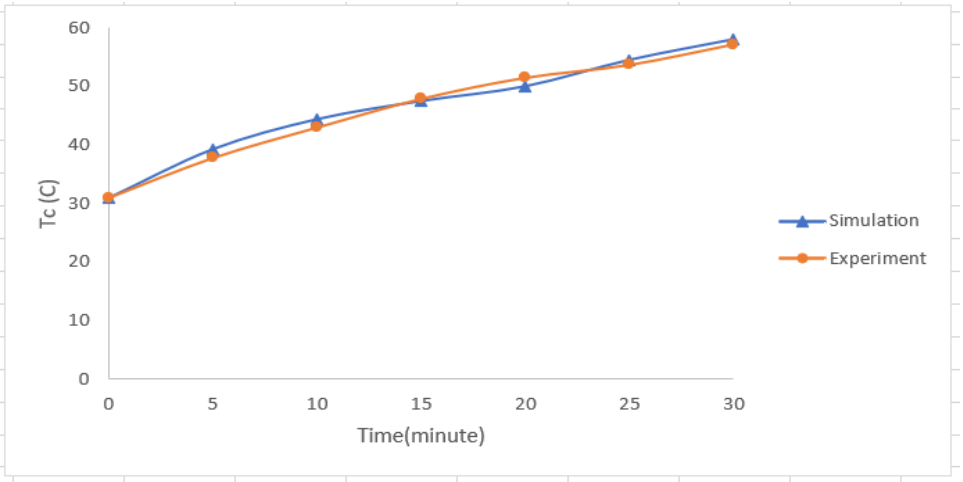

Fig. 5.8. Graph for the temperature analysis of microprocessor under load and fan off condition.

5.1. Simulation and Experimental Observations:

- From the above analysis deviations between the simulation and experiment is observed. The deviations may be due to the limitations of the software ANSYS 2023 R1 STUDENT version.
- It was observed that temperature was higher for both heat sinks under load condition compared to no load condition. Also, temperature was higher for heat sink 2 compared to heat sink 1 for both conditions. This is due to the fact that heat sink 1 is closer to CPU fan compared to heat sink 2.
- From the Figure 5.9 it is clear that large amount of air is flowing through heat sink 1 and for heat sink 2, total height is of the dimension 1.01cm from the base of CPU chassis such that only small amount of air flow through heat sink 2.
- So, heat sink 2 gets heated fast as compared to heat sink 1 as its dimension is 7.28cm.
- When obstacle was placed in between heat sink 1 and CPU fan, air flow was blocked and it can be observed that due to the obstacle the air flow became turbulent in between the region of obstacle and CPU fan.
- From the Figure 5.10 it is clear that amount of air flowing through heat sink 1 was reduced and small amount of air was flowing through heat sink 2.
- For fan off condition, small amount of air was flowing through the CPU fan opening with respect to surrounding environment which can be neglected. (Fig. 5.11 and Fig. 5.12)

- We have observed that removing the heat sink 1 and disconnecting the CPU fan causes further rise in temperature for the microprocessor under both no load and load conditions.

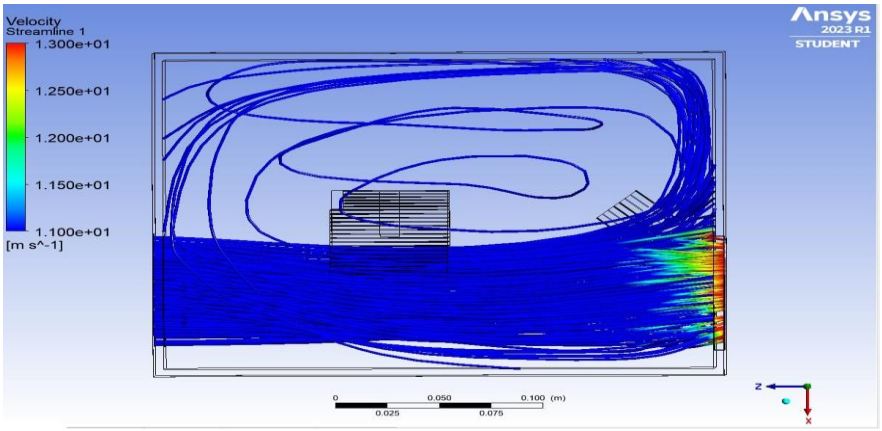

Fig. 5.9. Air flow pattern inside the CPU chassis from the CPU fan under no load and load condition

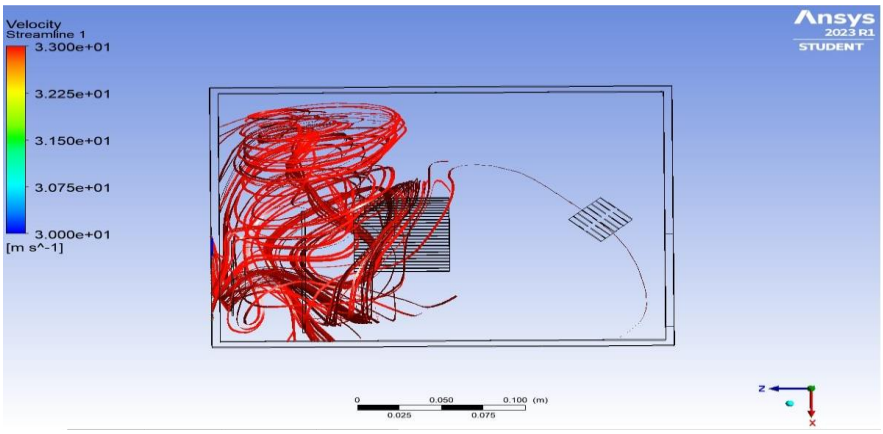

Fig. 5.10. Air flow pattern inside the CPU chassis from the CPU fan under no load and load condition, by placing an obstacle.

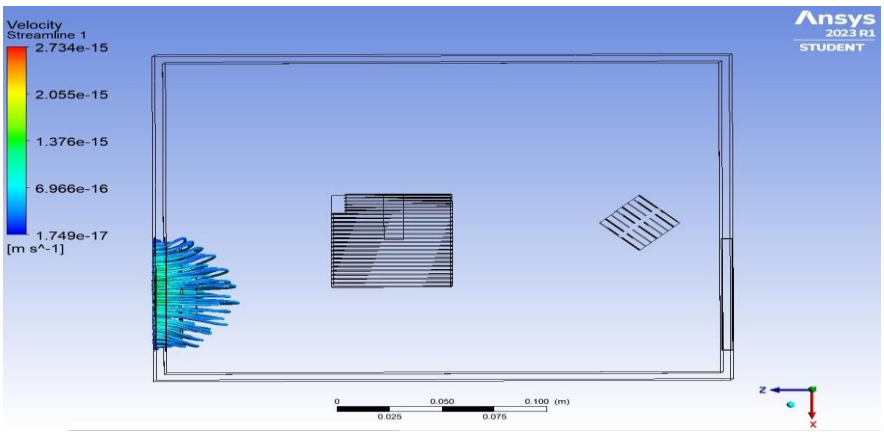

Fig. 5.11. Air flow pattern inside the CPU chassis from the CPU fan for fan off under no load and load condition.

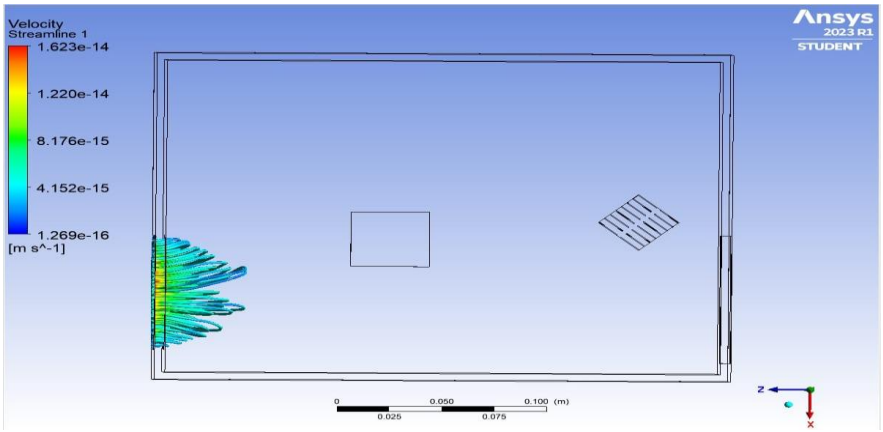

Fig. 5.12. Air flow pattern inside the CPU chassis from the CPU fan for fan off under no load and load condition on microprocessor.

CHAPTER 6

CONCLUSION

The research work presents detailed simulation and infrared thermographic study of heat sink and microprocessors under different no load and load conditions. Significant thermal differences have been observed under different conditions. Thermographic tools have shown as quite valuable to obtain detailed temperature distribution on these devices.

From the outcomes of the study, we can conclude the following points:

1) Heat generation on the microprocessor and heat sink depends on CPU utilization.
2) Heat gets dissipated from the microprocessor to heat sink through conduction and further dissipated from heat sink by convection.
3) Intel Core i7 processor series is installed and has an average maximum operating temperature range of 57^0C – 65^0C. Without the heat sink installed above the microprocessor and under the absence of fan, temperature rises up rapidly to 57.2^0C within short period of time, causing computer to shut down automatically in order to cool down and prevent further damage to the computer.
4) CPU fan and position, shape, dimension of heat sink and other factors related to it plays an important role in dissipating heat away from the microprocessor.
5) Numerical and Experimental analysis have been done which shows small deviations between them.
6) Future scope of the work is that implementing nano fluid pump instead of heat sink 1 over the microprocessor so that temperature can be reduced to an extent.
7) Proposed model for the future work has been designed as shown in Figure 6.1 and researcher can make any changes to the model's shape, dimension and position as per their convenience.

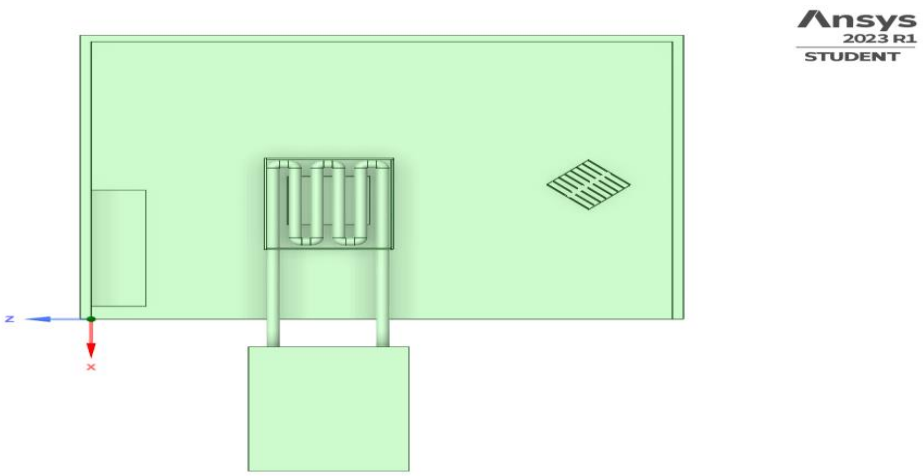

Fig. 6.1. Design of Nanofluid pump for future work

REFERENCES

[1] Lama Hamadeh, Amin Al-Habaibeh, Towards reliable smart textiles: Investigating thermal characterisation of embedded electronics in E-Textiles using infrared thermography and mathematical modelling, Sensors and Actuators 2022; 338:113501. https://doi.org/10.1016/j.sna.2022.113501

[2] Daiki Otaki, Hirofumi Nonaka, Noboru Yamada, Thermal design optimization of electronic circuit board layout with transient heating chips by using Bayesian optimization and thermal network model, International Journal of Heat and Mass Transfer 2022;184:122263. https://doi.org/10.1016/j.ijheatmasstransfer.2021.122263

[3] Hamid Maleki, Mohammad Reza Safaei, Arturo S. Leon, Improving shipboard electronics cooling system by optimizing the heat sinks configuration, Journal of Ocean Engineering and Science 2022;7:498-508. https://doi.org/10.1016/j.joes.2021.09.013

[4] Kai Zhuaa, Xueqiang Li, Hailong Li, Zhen Yang, Yabo Wang, Experimental investigation on the effect of heat sink temperature on operational characteristics of a new-type loop heat pipe, Energy Procedia 2019;158:2423 – 2429. https://doi.org/10.1016/j.egypro.2019.01.298

[5] A. Moure, A. Serrano, S Roman Sanchez, I. Lorite, J F Fernandez, Influence of the design on the thermal response of press-fit diodes: An infrared thermographic study, Results in Physics 2021;22:103909. https://doi.org/10.1016/j.rinp.2021.103909

[6] S R Sanchez, A. Serrano, I. Lorite, J F Fernandez, A. Moure, A del Campo, Thermal response of active Si in press-fit rectifier diodes by confocal Raman microscopy: Influence of diode design and technology, Journal of Materials Research and Technology 2022;18:2570 – 2581. https://doi.org/10.1016/j.jmrt.2022.03.116

[7] Adam Norman, Mark Gallina, Olena Zhu, Joyce Weiner, Fabian Garita Gonzalez, AI/ML Applications for thermally aware SoC Designs, ASME 2022 International Technical Conference and Exhibition on Packaging and Integration of Electronic and Photonic Microsystems 2022;1:97186. https://doi.org/10.1115/IPACK2022-97186

[8] Andrea Tilli, Emanuele Garone, Christian Conficoni, Mateo Cacciari, Alessandro Bosso, Andrea Bartolini, Two layer distributed model predictive control approach to thermal control of multiprocessor of system on chip, Journal of Control Engineering Practice 2022;122(1):105099. https://doi.org/10.1016/j.conengprac.2022.105099

[9] Ziqiang He, Yunfei Yan, Zhien Zhang, Thermal management and temperature uniformity enhancement of electronic devices by micro heat sink, Journal of Energy 2020;216:119223. https://doi.org/10.1016/j.energy.2020.119223

[10] Jinwei Zhang, Sheriff Sadiqbatcha, Liang Chen, Cuong Thi, Sachin Sachdeva, Hussam Amrouch, Sheldon X.-D.Tan, Hot spot aware thermoelectric array based cooling for multicore processors, Integration 2022;89;73 – 82. https://doi.org/10.1016/j.vlsi.2022.11.006

[11] Shuai Feng, Yunfei Yan, Haojie Li, Li Zhang, Shilin Yang, Thermal management of 3D chip with non - uniform hotspot by integrated gradient distribution annular cavity micro pin fin, Journal of Applied Thermal Engineering 2020;182:116132. https://doi.org/10.1016/j.applthermaleng.2020.116132

[12] Koji Nishi, Investigation regarding transient compact thermal model for microprocessor packages, ASME 2019 International Technical Conference and Exhibition on Packaging and Integration of Electronic and Photonic Microsystem 2019;1:6390. https://doi.org/10.1115/IPACK2019-6390

[13] George Oguntala, Raed Abd – Alhameed, Mohammed Ngala, Transient thermal analysis and optimization of convective – radiative porous fin under the influence of magnetic field for efficient microprocessor cooling, International Journal of Thermal Sciences 2019;145:1-11. https://doi.org/10.1016/j.ijthermalsci.2019.106019

[14] Aziz Oukaira, Ahmad Hassan, Mohamed Ali, Yvon Savaria, Ahmed Lakhssassi, Towards Real-Time Monitoring of Thermal Peaks in Systems-on-Chip (SoC), Sensors 2022;22:5904. https://doi.org/10.3390/s22155904

[15] Vladimir Ivanov, Sergey Smolentsev, Alexey Filyakov, Microprocessor temperature control device for a thermal object, E3S Web of Conferences 2022;363:01027. https://doi.org/10.1051/e3sconf/202236301027

[16] Pedro A.M.B, F Krismer, J. W. Kolar, R. K. Aljameh, S. Paredes, R. Heller, T. Brunschwiler, P. A. Francese, T. Morf, M. A. Kossel, M. Braendli, Electrical and Thermal

characterization of an inductor based ANPC-Type Buck converter in 14nm CMOS Technology for microprocessor applications, Open Journal of Power Electronics 2020;1:456 – 468. https://doi.org/10.1109/OJPEL.2020.3025658

[17] M Z I Bangalee, Md Mizanur Rahman, M Ferdows, M S Islam, Numerical Analysis of Thermal Convection in a CPU Chassis, Open Journal of Modelling and Simulation 2021;9:43 – 58. http://dx.doi.org/10.4236/ojmsi.2021.91003

[18] Alhassan Salami Tijani, Nursyameera Binti Jaffri, Thermal analysis of perforated pin fins heat sink under forced convection condition, International Conference on System Integrated Intelligence 2018;24:290 – 298. https://doi.org/10.1016/j.promfg.2018.06.025

[19] Songkran Wiriyasart, Chootichai Hommalee, Paisarn Naphon, Thermal cooling enhancement of dual processors computer with thermoelectric air cooler module, Case Studies in Thermal Engineering 2019;14:100445. https://doi.org/10.1016/j.csite.2019.100445

[20] A. Siricharoenpanich, S. Wiriyasrt, A Srichat, P Naphon, Thermal management of CPU cooling with a novel short heat pipe cooling system, Case Studies in Thermal Engineering 2019;15:100545. https://doi.org/10.1016/j.csite.2019.100545

[21] Q. Zhu, K. Chang, J. Chen, X. Zhang, H. Xia, H. Zhang, H. Wang, H. Li, Y. Jin, Characteristics of heat transfer and fluid flow in microchannel heat sinks with rectangular grooves and different shaped ribs, Alexandria Engineering Journal 2020;59:4593 – 4609. https://doi.org/10.1016/j.aej.2020.08.014

[22] Hussam Amrouch, Joohno Kong, Young Ho Gong, S. W. Chung, J. H. Choi, Young Seo Lee, Ji Heon Lee, Characterizing the Thermal Feasibility of Monolithic 3D Microprocessors, IEEE Access 2021;9:120715 – 120729. https://doi.org/10.1109/ACCESS.2021.3108628

[23] Subodha Charles, Prabhat Mishra, Lightweight Encryption and Anonymous Routing in NoC based SoCs, IEEE Access 2023;1:1 – 12. https://doi.org/10.48550/arXiv.2302.06118

[24] Zhongjie Lu, Mingjie Li, Chenlong Yang, Xiangqiang Cheng, Jianfei Zhan, Experimental and numerical study on the heat transfer and flow characteristics of micro-gap chip with longitudinal vortex generator array, Case Studies in Thermal Engineering, 2023;45:102979. https://doi.org/10.1016/j.csite.2023.102979